nature microbiology

Article

https://doi.org/10.1038/s41564-023-01383-1

Age-associated features of norovirus infection analysed in mice

Received: 17 June 2022

Accepted: 17 April 2023

Published online: 15 May 2023

Check for updates

Elizabeth A. Kennedy[1], Somya Aggarwal[1], Arko Dhar[1], Stephanie M. Karst[2], Craig B. Wilen[3] & Megan T. Baldridge[1,4]

Norovirus (NoV) is the leading global cause of viral gastroenteritis. Young children bear the highest burden of disease and play a key role in viral transmission throughout the population. However, which host factors contribute to age-associated variability in NoV severity and shedding are not well-defined. The murine NoV (MNoV) strain CR6 causes persistent infection in adult mice and targets intestinal tuft cells. Here we find that natural transmission of CR6 from infected dams occurred only in juvenile mice. Direct oral CR6 inoculation of wild-type neonatal mice led to accumulation of viral RNA in the ileum and prolonged shedding in the stool that was replication-independent. This viral exposure induced both innate and adaptive immune responses including interferon-stimulated gene expression and MNoV-specific antibody responses. Interestingly, viral uptake depended on passive ileal absorption of luminal virus, a process blocked by cortisone acetate administration, which prevented ileal viral RNA accumulation. Neonates lacking interferon signalling in haematopoietic cells were susceptible to productive infection, viral dissemination and lethality, which depended on the canonical MNoV receptor CD300LF. Together, our findings reveal developmentally associated aspects of persistent MNoV infection, including distinct tissue and cellular tropism, mechanisms of interferon regulation and severity of infection in the absence of interferon signalling. These emphasize the importance of defining viral pathogenesis phenotypes across the developmental spectrum and highlight passive viral uptake as an important contributor to enteric infections in early life.

Norovirus (NoV) is the leading cause of acute gastroenteritis worldwide, affecting individuals of all ages but causing particularly high morbidity and mortality in children younger than five. Young children bear the highest burden of disease[1], with 66–90% experiencing at least one NoV infection before age three[2]. They often exhibit more prolonged and higher levels of faecal viral shedding than older children or adults[3,4], contributing to their central role in viral transmission to all age groups[5]. Although no vaccines or treatments for NoV currently exist, development of therapies targeting persistent NoV shedding in children could reduce faecal-oral spread throughout the entire population.

Murine NoV (MNoV) is a natural mouse pathogen that shares features with human NoVs including faecal-oral transmission, mechanisms of genome replication and virion structure, serving as a powerful model for in vivo studies of pathogenesis[6]. Different MNoV strains model different aspects of human NoV infection. Acute

[1]Division of Infectious Diseases, Department of Medicine, Edison Family Center for Genome Sciences and Systems Biology, Washington University School of Medicine, St Louis, MO, USA. [2]Department of Molecular Genetics and Microbiology, College of Medicine, University of Florida, Gainesville, FL, USA. [3]Departments of Laboratory Medicine and Immunobiology, Yale School of Medicine, New Haven, CT, USA. [4]Department of Molecular Microbiology, Washington University School of Medicine, St Louis, MO, USA. e-mail: mbaldridge@wustl.edu

strains infect gut-associated haematopoietic cells and are cleared by 7–14 d post-infection (dpi) in wild-type mice[7,8]. Conversely, persistent strains infect rare intestinal epithelial tuft cells and are shed in faeces of wild-type animals through at least 70 dpi (refs. 9,10), modelling human persistent asymptomatic shedding. All MNoV strains tested so far use the host protein CD300LF as a receptor[11–13]. Interferons (IFNs) are central for innate immune control of MNoV, with type III IFNs limiting intestinal viral replication and type I IFNs limiting viral dissemination to systemic tissues[14–17] and pathogenesis of acute strains[18]. Importantly, most studies characterizing MNoV pathogenesis have used adult mice, although NoV is an important cause of paediatric gastroenteritis.

It was recently reported that wild-type neonatal mice develop diarrhoea after infection with an acute strain of MNoV, whereas persistent strains of MNoV cause substantially less diarrhoea[19,20]. Whether persistent MNoV contributes to ongoing shedding in neonates remains unknown. To develop a model of persistent paediatric infection, we examined the dynamics and host factors involved in neonatal infection with persistent MNoV strain CR6. We found that transmission from infected dams to naïve pups occurs after postnatal day (P)16. However, after direct inoculation at P6, viral genomes are detected in stool until 10 dpi. Intriguingly, in wild-type neonates, viral RNA is uniquely detected in ilea, and viral RNA presence is largely independent of tuft cells or CD300 viral receptors, both of which are required for CR6 infection of adults. Viral RNA ileal uptake and faecal shedding are unaffected by antiviral treatment but blocked by cortisone, which limits non-specific uptake in the neonatal ileum. In contrast, when types I and II IFN signalling are disrupted, specifically in haematopoietic cells, CD300-dependent viral dissemination and lethality follow neonatal CR6 inoculation. Our data demonstrate passive ileal absorption as an understudied mechanism for enteric viral uptake in neonates, which is counterbalanced by host IFN signalling in haematopoietic cells to limit dissemination.

Results

Natural transmission of CR6 occurs after postnatal day 16

We initially investigated transmission of MNoV strain CR6 from infected dams to their naïve litters before weaning at P21. Most pups did not shed viral RNA early in life, but almost all began shedding in the transition from P16 to P21 (Fig. 1a,b). CR6 was not detectable in ilea or colons of pups at P6 or P13, but was present at P21 (Fig. 1c,d). Transmission between P16 and P21 is consistent with the age at which pups become coprophagic[21] and could be naturally infected from the dam's stool.

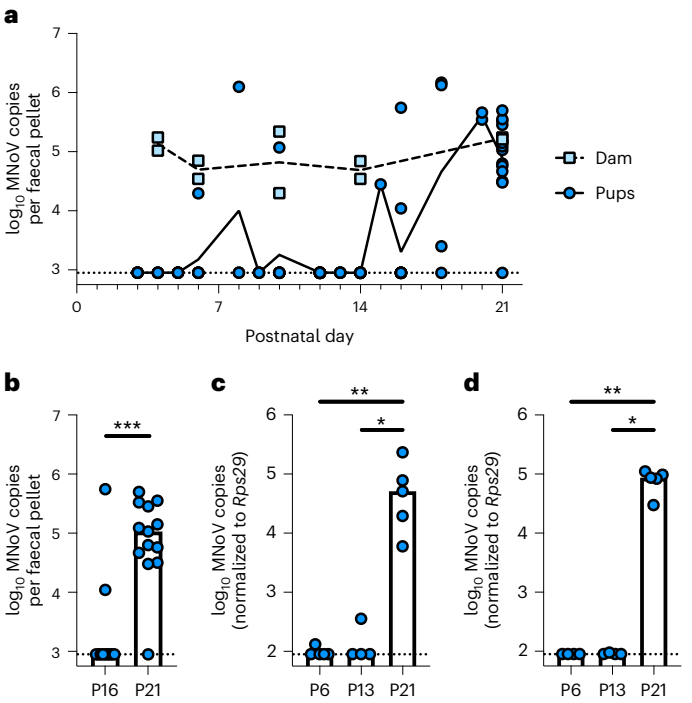

Fig. 1 | Natural transmission of persistent MNoV from infected dams occurs after P16. Pregnant C57BL/6 dams were orally inoculated with CR6 5–6 d before giving birth. **a**–**d**, Faecal samples were collected from pups up to P21 and MNoV genome copies detected by real-time quantitative reverse transcription PCR (RT-qPCR). **b** is a comparison of P16 and P21 faecal samples from **a**. Ileum (**c**) and colon (**d**) samples were collected and MNoV genome copies detected by RT-qPCR. Data were analysed using two-tailed Mann-Whitney test (**b**) or Kruskal-Wallis test with Dunn's multiple comparisons (**c**,**d**). For **a**, $n = 22$ pups from 3 litters. Given the challenge of obtaining stool from young mice, faecal samples were collected as possible; each data point indicates stool from a single mouse, with exact n for each timepoint indicated in Source Data. In **b**, $n = 11$ for P16 and $n = 13$ for P21; ***$P = 0.009$. For **c** and **d**, samples from 2 litters were collected at P6 ($n = 5$), P13 ($n = 4$) and P21 ($n = 5$); (**c**) *$P = 0.0204$, **$P = 0.0073$; (**d**) *$P = 0.0251$, **$P = 0.0072$. Dashed lines indicate limit of detection for assays.

CR6 inoculation is associated with age-dependent tissue tropism

To directly assess early-life infection, we orally inoculated mice with CR6 at P6 (neonates), P15 (juveniles) or between 6–9 weeks of age (adults). All inoculated mice shed viral RNA in their faeces between 3–10 dpi, with neonates shedding significantly more than juveniles or adults at early timepoints (Fig. 2a–c). At 7 dpi, ileal viral RNA was comparable among mice inoculated at different ages, although it trended lower in juvenile mice ($P = 0.1187$ vs adults, $P = 0.0842$ vs neonates) (Fig. 2d). Viral RNA was nearly undetectable in neonatal colons, in contrast to substantial colonic viral RNA in juveniles and adults, suggesting age-dependent differences in CR6 localization (Fig. 2e).

Intestinal microbiota composition varies between mice from different vendors[22] or different genetic backgrounds[23]. Because commensal bacteria promote persistent MNoV infection of adult mice[24], we compared CR6 faecal shedding from C57BL/6 neonates sourced from Charles River (CR), Jackson Laboratories (JAX) or bred at Washington University in St Louis (WUSTL). JAX neonates shed more viral RNA than WUSTL or CR neonates (Extended Data Fig. 1a). Among a variety of genetic backgrounds sourced from JAX, C57BL/6 shed at the highest levels (Extended Data Fig. 1b). BALB/c are more susceptible to rotavirus than C57BL/6 neonates[25], and both are susceptible to diarrhoea after infection with acute MNoV strains[19,20]. While ileal and stool CR6 RNA were comparable between BALB/c and C57BL/6 pups at 7 dpi, BALB/c pups exhibited higher colonic viral RNA (Extended Data Fig. 1c,d). Interestingly, adult BALB/c mice exhibited decreased stool viral RNA and trended towards decreased intestinal viral RNA (Extended Data Fig. 1e,f). Genetic background and microbiota may thus differentially influence CR6 localization throughout life.

Tuft cells are dispensable for neonatal CR6 RNA shedding

Intestinal tuft cells are the target of persistent CR6 infection in adult mice[10]. We inoculated neonatal and juvenile *Pou2f3*$^{-/-}$ mice, which lack tuft cells[26], and found that faecal shedding of CR6 RNA was independent of tuft cells in neonates (Fig. 3a), but dependent on tuft cells in juveniles (Fig. 3b). The dynamics of tuft cell development remain unclear, as some studies suggest that tuft cells develop prenatally[27], while others report that they do not accumulate until weaning[28]. In our mice, tuft cells (quantified by staining for marker DCLK1) were rare at P6 and P13 (Fig. 3c,d and Extended Data Fig. 2a). By P21, tuft cells remained rare in ileum but reached adult-like levels in colon. Co-staining for MNoV non-structural protein NS6/7 showed no CR6-positive tuft cells at 7 dpi in neonates, compared with detectable co-localization in adults (Fig. 3e). We similarly failed to observe non-tuft NS6/7-positive cells in the neonatal ileum. Altogether, our findings suggest that intestinal tuft cells are rare during early life and neonatal CR6 RNA shedding is independent of tuft cells.

https://doi.org/10.1038/s41564-023-01383-1

CD300LF is largely dispensable for neonatal CR6 RNA shedding

In adult mice, CD300LF expression on tuft cells is required for CR6 infection[8,12,13]. Among intestinal epithelial cells (IECs), CD300LF is expressed exclusively on tuft cells[10,29], but cells including macrophages and dendritic cells express CD300LF and are permissive to other MNoV strains[8]. *Cd300lf* expression in the colon was low early in life, but reached adult-like levels by P21, mirroring colonic tuft cell development (Extended Data Fig. 2b). In contrast, ileal *Cd300lf* expression was age-independent, suggesting that non-tuft cells expressing CD300LF could support CR6 RNA shedding. *Cd300lf*$^{-/-}$ mice shed viral RNA after neonatal but not after juvenile inoculation (Figs. 3a,b), although *Cd300lf*$^{-/-}$ neonates shed less viral RNA than wild-type neonates (Fig. 3a) and exhibited decreased viral RNA in mesenteric lymph nodes (MLNs) and spleen but not in ilea (Fig. 3f), suggesting a partial role for CD300LF in neonatal viral RNA uptake. To confirm this, we pre-incubated CR6 with Fc-fusion proteins with either the mouse CD300LF ectodomain (Fc-msCD300LF), which neutralizes MNoV[30], or a human CD300LF ectodomain control (Fc-huCD300LF)[13]. Fc-msCD300LF, but not Fc-huCD300LF, blocked CR6 infection of BV2 microglia cells in vitro (Extended Data Fig. 3). Neonates inoculated with CR6 pre-incubated with Fc-msCD300LF exhibited reduced CR6 RNA shedding (Fig. 3g) and intestinal viral RNA (Fig. 3h), although substantial viral RNA remained detectable in stool and ilea. These data support the idea that CD300LF is partially involved in, but not necessary for, neonatal CR6 RNA uptake and shedding.

We hypothesized that another CD300 family member, CD300LD, may be involved in neonatal viral RNA shedding as CD300LD expression permits MNoV infection in vitro[11,12]. We found that *Cd300lf*$^{-/-}$*Cd300ld*$^{-/-}$ neonates shed viral RNA comparable to *Cd300lf*$^{-/-}$ neonates (Fig. 3a), whereas juvenile mice shed no virus (Fig. 3b). Thus, CD300LD is not responsible for CD300LF-independent early life viral RNA release.

STAT1 controls CR6 lethality and dissemination in neonates

In adult mice, CR6 replication is controlled by innate immune responses, particularly IFN pathways[15]. In contrast, neonatal *Rag1*$^{-/-}$ mice lacking B and T cells have higher viral titres after infection with acute MNoV strains, indicating adaptive immune control[19]. Neonatal CR6 inoculation induced IFN-stimulated genes *Ifit1* and *Mx2* in the ileum at 1 and 7 dpi (Fig. 4a,b and Extended Data Fig. 4a,b), an induction not observed in colon (Extended Data Fig. 4c). Additionally, CR6-inoculated neonates generated serum anti-MNoV immunoglobulin (Ig)M and IgG responses at 14 dpi (Fig. 4c,d), demonstrating that both innate and adaptive immune systems respond to neonatal inoculation. To test the contribution of innate and adaptive immunity in CR6 control, we infected *Stat1*$^{-/-}$ (lacking a key transcription factor in IFN signalling) and *Rag1*$^{-/-}$ neonates. Faecal shedding in both was equivalent to wild-type neonates at 7 dpi (Fig. 4e). Unexpectedly, *Stat1*$^{-/-}$ neonates succumbed to infection with CR6, exhibiting ~75% lethality by 14 dpi (Fig. 4f). This contrasts with adult *Stat1*$^{-/-}$ mice, which rarely die after CR6 infection[31,32]. No lethality was observed in *Rag1*$^{-/-}$ neonates, suggesting that regulation of viral pathogenesis is specific to IFN responses rather than altered priming of adaptive responses.

We next asked which type(s) of IFN limit CR6-associated neonatal lethality. Neonates lacking *Ifnar1*, *Ifngr1* or *Ifnlr1*, necessary for type I, II and III IFN signalling, respectively, did not succumb to infection (Fig. 4g). In adult mice, type I and II IFNs combinatorially limit lethality after acute MNoV infection[33], and indeed *Ifnar1*$^{-/-}$*Ifngr1*$^{-/-}$ neonates succumbed to CR6 infection (Fig. 4g). We also sought to define the cell type(s) in which *Stat1* expression prevents CR6 lethality. *Villin-Cre+;Stat1*$^{f/f}$ and *Lysm-Cre+;Stat1*$^{f/f}$ neonates, which lack *Stat1* expression in epithelial and myeloid cells, respectively, survived infection (Fig. 4h). In contrast, *Vav-iCre+;Stat1*$^{f/f}$ neonates, lacking *Stat1* in haematopoietic and tuft cells, exhibited increased lethality versus littermate controls (Fig. 4h). Adult *Stat1*$^{-/-}$ mice exhibited increased intestinal and extraintestinal virus after CR6 infection[32]. Similarly, intestinal virus levels were higher in *Stat1*$^{-/-}$ versus wild-type neonates, and

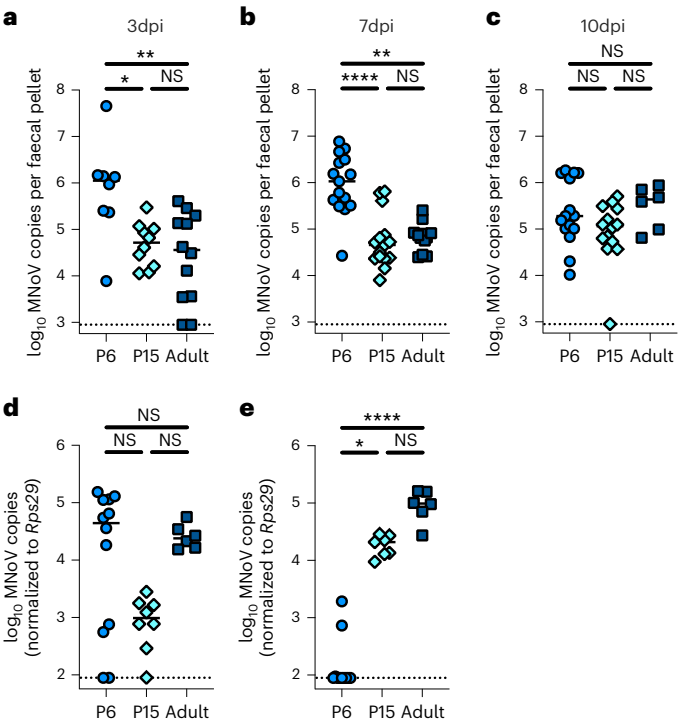

Fig. 2 | Inoculation of pups with persistent MNoV is associated with distinct localization. C57BL/6 mice were orally inoculated with CR6 at P6, P15 or as adults (6–9 weeks old). **a**–**e**, Faecal samples were collected at 3 dpi (**a**), 7 dpi (**b**) and 10 dpi (**c**), and MNoV genome copies detected by RT-qPCR. Ileum (**d**) and colon (**e**) samples were collected at 7 dpi and MNoV genome copies detected by RT-qPCR. Data were analysed using one-way analysis of variance (ANOVA) with Holm-Šídák's multiple comparisons test (**a**) or Kruskal-Wallis test with Dunn's multiple comparisons (**b**–**e**). In **a**, P6 $n = 8$, 3 litters; P15 $n = 10$, 2 litters; adult $n = 12$, 2 independent experiments; $^{*}P = 0.0160$, $^{**}P = 0.0033$. NS, not significant ($P > 0.05$). In **b**, P6 $n = 15$, 4 litters; P15 $n = 15$, 3 litters; adult $n = 12$, 3 independent experiments; $^{**}P = 0.0034$, $^{****}P < 0.0001$. In **c**, P6 $n = 15$, 5 litters; P15 $n = 14$, 3 litters; adult $n = 6$, 2 independent experiments. In **d** and **e**, P6 $n = 12$, 2 litters; sourced from Charles River; P15 $n = 8$, 2 litters; adult $n = 6$, 2 independent experiments; $^{*}P = 0.0193$, $^{****}P < 0.0001$. Dashed lines indicate limit of detection for assays.

virus disseminated to extraintestinal sites in *Stat1*$^{-/-}$ neonates (Fig. 4i). Intestinal and systemic viral RNA were also higher in *Vav-iCre+;Stat1*$^{f/f}$ neonates compared with littermates (Fig. 4j). Additionally, we detected enhanced CR6 RNA in *Stat1*$^{-/-}$ ilea using RNA in situ hybridization (RNA-ISH) (Fig. 4k). Together, these data suggest that type I and II IFN signalling, acting at least partly in haematopoietic cells, limit viral replication, dissemination and lethality after neonatal CR6 inoculation.

We also assessed whether CR6 pathogenesis in *Stat1*$^{-/-}$ mice was CD300-dependent. *Stat1*$^{-/-}$*CD300lf*$^{-/-}$ and *Stat1*$^{-/-}$*CD300lf*$^{-/-}$*Cd300ld*$^{-/-}$ neonates inoculated with CR6 exhibited significantly reduced lethality compared with *Stat1*$^{-/-}$ neonates (Fig. 4l), with reduced intestinal viral RNA and no detectable dissemination to spleen or brain (Fig. 4m). CR6 dissemination and pathogenesis in *Stat1*$^{-/-}$ neonates is thus CD300 receptor-dependent. Intriguingly, substantial viral RNA was still present in *Stat1*$^{-/-}$*CD300lf*$^{-/-}$ and *Stat1*$^{-/-}$*CD300lf*$^{-/-}$*Cd300ld*$^{-/-}$ ilea (Fig. 4m), and faecal viral RNA was comparable to that in *Stat1*$^{-/-}$ mice (Fig. 4n), similar to observations in *Cd300lf*$^{-/-}$ and *Cd300lf*$^{-/-}$*Cd300ld*$^{-/-}$ neonates (Fig. 3a,f). We therefore sought to further characterize the ileal and stool CR6 RNA in neonatal mice.

CR6 replicates in *Stat1*$^{-/-}$ but minimally in wild-type neonates

To delineate the nature of CD300-independent CR6 RNA shedding in neonates, we treated mice with viral polymerase inhibitor 2′-C-methylcytidine (2-CMC), which limits CR6 replication and

https://doi.org/10.1038/s41564-023-01383-1

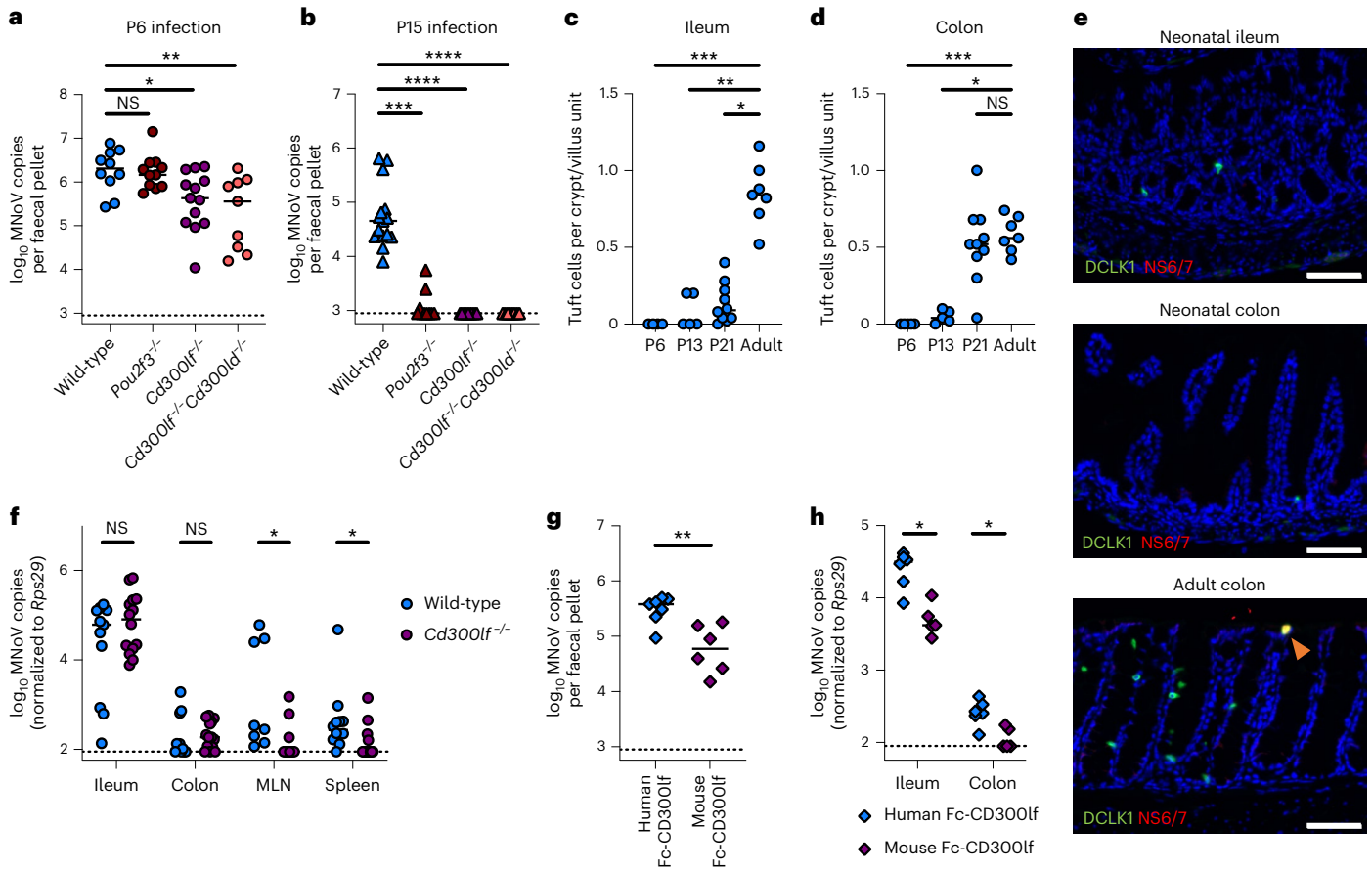

Fig. 3 | Tuft cells and CD300 family viral receptors have a limited role in neonatal viral RNA shedding. a,**b**, Mice were orally inoculated with CR6 at P6 (**a**) or P15 (**b**) and MNoV genome copies quantified from 7 dpi stool samples by RT-qPCR. **c**,**d**, Tuft cells were quantified by immunofluorescent staining of DCLK1 in ileum (**c**) and colon (**d**) of naïve wild-type mice. **e**, Intestinal samples from mice orally inoculated with CR6 at P6 (neonatal) or as adults were collected at 7 dpi and stained for DCLK1 and CR6 non-structural protein NS6/7. Orange arrowhead indicates a CR6-infected tuft cell. Scale bars, 30 µm. **f**, Neonates were orally inoculated with CR6 at P6 and MNoV genome copies quantified from 7 dpi samples by RT-qPCR. **g**,**h**, CR6 was pre-incubated with Fc-huCD300lf or Fc-msCD300lf before oral inoculation of C57BL/6 littermates at P6. Stool (**g**) and tissue (**h**) virus levels were quantified by RT-qPCR at 7 dpi. Data were analysed using one-way ANOVA with Holm-Šídák multiple comparisons (**a**), Kruskal-Wallis test with Dunn's multiple comparisons (**b**–**d**), two-tailed Mann-Whitney test corrected with the Holm-Šídák method (**f**,**h**) or two-tailed *t*-test (**g**). In **a**, wild-type $n = 10$, 3 litters; *Pou2f3*$^{-/-}$ $n = 11$, 2 litters; *Cd300lf*$^{-/-}$ $n = 13$, 4 litters; and *Cd300lf*$^{-/-}$*Cd300ld*$^{-/-}$ $n = 9$, 2 litters; $^{*}P = 0.0235$, $^{**}P = 0.0046$. In **b**, wild-type $n = 15$, 3 litters; *Pou2f3*$^{-/-}$ $n = 10$, 3 litters; *Cd300lf*$^{-/-}$ $n = 11$, 2 litters; and *Cd300lf*$^{-/-}$ *Cd300ld*$^{-/-}$ $n = 11$, 3 litters; $^{***}P = 0.0001$ (wild-type vs *Pou2f3*$^{-/-}$), $^{****}P < 0.0001$ (wild-type vs *Cd300lf*$^{-/-}$ and wild-type vs *Cd300lf*$^{-/-}$*Cd300ld*$^{-/-}$). Wild-type 7 dpi data overlaps with P6/P15 litters in Fig. 2b. In **c** and **d**, P6 $n = 5$; P13 $n = 5$; P21 $n = 10$; adult $n = 7$, each from 2 independent experiments. In **c**, $^{*}P = 0.0173$, $^{**}P = 0.0042$, $^{***}P = 0.0003$. In **d**, $^{*}P = 0.0257$, $^{***}P = 0.0009$. In **e**, representative of 4 samples for neonatal ileum and colon. In **f**, wild-type $n = 12$, 2 litters (sourced from Charles River) or *Cd300lf*$^{-/-}$ $n = 14$, 2 litters; $^{*}P = 0.0185$ (MLN, spleen). Wild-type ileum/colon data overlaps with Fig. 2d,e. In **g**,**h**, Fc-huCD300lf $n = 7$ and Fc-msCD300lf $n = 6$ from 2 litters. In **g**, $^{**}P = 0.0036$. In **h**, $^{*}P = 0.0172$ (ileum), $^{*}P = 0.0173$ (colon). Dashed lines indicate limit of detection for assays.

shedding in adult mice (Extended Data Fig. 5)[34]. 2-CMC treatment beginning at 3 dpi protected *Stat1*$^{-/-}$ neonates from lethality (Fig. 5a). While we were unable to directly compare tissue viral levels within these experiments, as untreated mice succumbed to infection by 7 dpi, we observed lower viral RNA in 2-CMC-treated *Stat1*$^{-/-}$ neonates across tissues compared with previous experiments (compared to Fig. 4i; average $1 \times 10^{4.1}$ in untreated versus $1 \times 10^{2.4}$ brain MNoV genome copies in 2-CMC-treated mice), suggesting that 2-CMC limits CR6 dissemination in *Stat1*$^{-/-}$ neonates (Fig. 5b). However, stool viral RNA in *Stat1*$^{-/-}$ neonates was unaffected by 2-CMC treatment (Fig. 5c). Similarly, 2-CMC treatment beginning at 3 dpi did not reduce ileal or stool viral RNA in wild-type mice at 7 dpi. When antiviral treatment began at 0 dpi, ileal and stool viral RNA decreased subtly but remained detectable (Fig. 5d,e). Thus, while CR6 may replicate immediately after inoculation in wild-type neonates, viral RNA in the ileum and stool at later timepoints is predominantly independent of viral replication.

We questioned whether the detected virus was infectious, as viral nucleic acids may be shed in the absence of infectious virus[35]. While tissues and stool from adult mice produced plaques on BV2 cells in vitro, no plaques were detected from samples of wild-type neonates at 3–10 dpi (Fig. 5f,g). Neonatal stool (1 and 2 dpi) produced plaques, consistent with passage of infectious inoculum (Extended Data Fig. 6a). Samples from *Stat1*$^{-/-}$ neonates produced plaques (Fig. 5h,i), suggesting that infectious virus is produced in neonates lacking IFN signalling. Additionally, double-stranded (ds) RNA and MNoV non-structural viral protein NS6/7 co-localized with CD45 in spleen from *Stat1*$^{-/-}$ neonates, supporting viral replication in haematopoietic cells (Fig. 5j and Extended Data Fig. 6b–d). Together, these data suggest that IFNs limit production of infectious CR6 in neonates, and CR6 RNA detected in ilea and stool of immunocompetent neonates is not due to replicative infection.

CR6 does not persistently infect mice inoculated as neonates

We next assessed how long viral RNA remained detectable in the stool of mice inoculated as neonates. At 14 dpi, CR6 RNA presence in stool depended on the infection status of the litter's dam (Fig. 5k). As the

dam was not directly inoculated, maternal infection probably occurred via coprophagy early after pup inoculation, and infected dams could transfer virus to pups after P16 as in Fig. 1. Without maternal infection, neonates generally shed no faecal viral RNA at 14 dpi. Similarly, *Cd300lf*$^{-/-}$ neonates largely cleared faecal viral RNA by 14 dpi (Fig. 5l). These data suggest that early-life CR6 inoculation does not lead to persistent infection without secondary transmission from infected dams.

Finally, to identify the source of viral RNA in wild-type neonatal stool, we assessed IEC extrusion, which is induced by rotavirus infection in neonatal mice[36]. We quantified expression of murine housekeeping gene *Rps29* in faecal samples of CR6-inoculated mice. CR6 inoculation increased IEC extrusion in adult but not in neonatal mice (Fig. 5m). However, extrusion was markedly higher in P13 neonates than in P20 or adult mice. CR6 RNA in neonatal stool may thus originate from extruded IECs.

CR6 RNA accumulates in neonates by non-specific uptake

Persistent detection of CR6 RNA in neonatal ilea and stool raised the possibility of prolonged transit time. Adult mice gavaged with Evans blue dye clear dye by 24 h (Extended Data Fig. 7a)[24]. Conversely, neonates had visibly blue stool at 24 h post-gavage and only cleared dye by 72 h (Extended Data Fig. 7b), suggesting delayed transit time in neonates. However, since CR6 RNA was detectable up to 10 dpi (Fig. 2c), reduced transit time did not fully explain prolonged shedding. Interestingly, wild-type neonatal ilea were visibly blue at 7 dpi (Extended Data Fig. 7c), suggesting that the ileum retained inoculum. Enterocytes in the neonatal ileum internalize luminal material via non-specific endocytosis, a process which ceases by weaning[37,38]. We detected viral RNA in the epithelium of distal but not proximal small intestine of CR6-inoculated neonates (Fig. 6a and Extended Data Fig. 8). These data suggest that viral inoculum is taken up, potentially via non-specific endocytosis, into neonatal ileal IECs.

Neonatal uptake of luminal material is mediated by the endocytic machinery, including adapter protein DAB2 (ref. 37). Ileal *Dab2* expression was high at P6 and P13 but dropped by P21 (Fig. 6b), consistent with when neonatal ileal macromolecule uptake ceases in rodents[38]. Similarly, lysosomal enzyme *N*-acetylgalactosaminidase (*Naga*, involved in early-life macromolecule uptake[39]), transcriptional repressor *Blimp1*/*Prdm1* (regulates intestinal maturation[39,40]) and sucrase isomaltase (*Sis*, involved in transition to solid food consumption[39,40]) exhibited a profound transition between P13 and P21 (Extended Data Fig. 7d–f).

In neonatal rats, treatment with the steroid cortisone acetate blocks non-specific uptake by driving premature maturation of the intestinal epithelium[41]. Cortisone treatment decreased ileal *Dab2* expression (Fig. 6b) and conferred adult-like expression of *Naga*, *Prdm1* and *Sis* (Extended Data Fig. 7d–f), consistent with premature maturation of the neonatal mouse intestine. Ileal Evans blue retention was blocked by cortisone treatment (Extended Data Fig. 7c) and indeed, cortisone treatment of wild-type neonates decreased ileal CR6 RNA levels at 7 dpi (Fig. 6c), although it did not affect stool viral RNA levels (Fig. 6d). Intriguingly, cortisone treatment of *Cd300lf*$^{-/-}$ neonates decreased both ileal and stool viral RNA at 7 dpi, suggesting that a combinatorial effect of viral receptor and non-specific uptake or early infection may contribute to ongoing faecal shedding (Fig. 6e,f). Blocking virus uptake with cortisone treatment in wild-type neonates decreased ileal IFN-stimulated gene expression at 1 and 7 dpi (Fig. 6g,h), although whether this effect was secondary to decreased viral RNA or indirect immunosuppressive effects of steroids remains to be determined. Further, cortisone treatment increased serum anti-MNoV IgM and decreased anti-MNoV IgG, suggesting that it may inhibit class switching and IgG responses to inoculum (Fig. 6i,j). Cortisone treatment of adult mice did not alter stool or tissue CR6 levels, suggesting that steroid administration does not modulate viral susceptibility independent of effects on neonatal non-specific uptake (Extended Data Fig. 9). These findings support the idea that viral RNA in wild-type neonatal ilea is largely due to non-specific uptake of inoculum.

Discussion

Here we discovered intriguing developmental differences contributing to dramatically changed outcomes between neonatal and juvenile or adult mice after inoculation with persistent MNoV. In early life, intact IFN signalling and an absence of tuft cells contribute to resistance to persistent MNoV. However, neonates retain viral RNA input in the absence of productive infection via non-specific endocytosis of inoculum by enterocytes.

Because faecal-oral transmission is the dominant means of interhost transmission for persistent MNoV, natural transmission

Fig. 4 | STAT1 signalling protects against lethality and extraintestinal CR6 spread in neonatal mice. a–**d**, Wild-type neonates were orally inoculated with CR6 at P6. *Ifit1* was quantified by RT-qPCR from ilea collected at 1 (**a**) or 7 dpi (**b**) and compared to uninfected mice. Serum was collected at 14 dpi and anti-MNoV IgM (**c**) and IgG (**d**) quantified by ELISA and compared to mock-infected mice. **e**–**g**, Neonates were orally inoculated with CR6 at P6 and MNoV genome copies quantified from 7 dpi stool samples by RT-qPCR, with wild-type stool as shown in Fig. 2b (**e**). **f**,**g** Survival tracked through 14 dpi with wild-type survival curve replicated in **f** and **g**. **h**, Littermates for each Cre line, born to Cre− dams bred to Cre+ sires, were orally inoculated with CR6 at P6 and survival tracked through 14 dpi. **i**, Neonates were orally inoculated with CR6 at P6 and tissues collected at 7 dpi unless pups appeared ill and needed to be euthanized (5–6 dpi). Tissue MNoV genome copies were quantified by RT-qPCR. **j**, Littermates were orally inoculated with CR6 at P6 and tissue MNoV genome copies quantified at 6–7 dpi. **k**, Neonates were orally inoculated with CR6 at P6. Ilea were collected at 6–7 dpi and stained for CR6 RNA using RNA in situ hybridization. Scale bars, 50 µm. **l**–**n**, Neonates were orally inoculated with CR6 at P6 and survival tracked through 14 dpi, with *Stat1*$^{-/-}$ survival curve replicated from **f** (**l**). Tissues were collected at 5–7 dpi (**m**) and stool collected at 7 dpi (**n**) and MNoV genome copies quantified by RT-qPCR, with *Stat1*$^{-/-}$ tissues and stool as in **i** and **e**, respectively. Data were analysed using two-tailed *t*-test (**a**–**c**), two-tailed Mann-Whitney test (**d**), Welch's ANOVA (**e**), Gehan-Breslow-Wilcoxon test (**f**–**h**, **l**), two-tailed Mann-Whitney test corrected with the Holm-Šídák method (**i**,**j**) and Kruskal-Wallis test with Dunn's multiple comparisons (**m**,**n**). In **a**, naïve $n = 5$, 1 litter; infected $n = 6$, 3 litters; $^{*}P = 0.0114$. In **b**, naïve $n = 5$, 2 litters; infected $n = 13$, 4 litters; $^{*}P = 0.0171$. In **c** and **d**, mock-infected $n = 8$, 2 litters; infected $n = 11$, 4 litters; $^{*}P = 0.0153$ (**c**); $^{**}P = 0.0016$ (**d**). In **e**, wild-type $n = 15$, 4 litters; *Stat1*$^{-/-}$ $n = 12$, 5 litters; and *Rag1*$^{-/-}$ $n = 5$, 1 litter. In **f**, wild-type $n = 21$, 4 litters; *Stat1*$^{-/-}$ $n = 34$, 5 litters; and *Rag1*$^{-/-}$ $n = 13$, 2 litters; $^{****}P < 0.0001$. In **g**, wild-type $n = 21$, 4 litters; *Ifnar1*$^{-/-}$ $n = 21$, 4 litters; *Ifngr1*$^{-/-}$ $n = 18$, 3 litters; *Ifnlr1*$^{-/-}$ $n = 24$, 4 litters; and *Ifnar1*$^{-/-}$*Ifngr1*$^{-/-}$ $n = 22$, 4 litters; $^{****}P < 0.0001$. In **h**, *Villin-Cre-*;*Stat1*$^{f/f}$ $n = 9$; *Villin-Cre+*;*Stat1*$^{f/f}$ $n = 10$, littermates from 3 litters; *Lysm-Cre-*;*Stat1*$^{f/f}$ $n = 7$; *Lysm-Cre +* ;*Stat1*$^{f/f}$ $n = 12$, littermates from 3 litters; *Vav-iCre-*;*Stat1*$^{f/f}$ $n = 14$; *Vav-iCre+*;*Stat1*$^{f/f}$ $n = 12$, littermates from 4 litters; $^{*}P = 0.0210$. In **i**, wild-type $n = 18$, 3 litters (brain collected from 6 neonates from 1 litter); and *Stat1*$^{-/-}$ $n = 12$, 3 litters; $^{**}P = 0.0014$ (ileum), $^{****}P < 0.0001$ (duodenum, colon, MLN, spleen, liver, brain). In **j**, *Vav-iCre+*;Stat1$^{f/f}$ $n = 7$; *Vav-iCre+*;*Stat1*$^{f/f}$ $n = 15$ littermates from 3 litters; $^{*}P = 0.0248$ (ileum), $^{**}P = 0.0046$ (colon), $^{**}P = 0.0058$ (spleen), $P = 0.0521$ (brain). **k**, Representative of $n = 5$ wild-type ilea, $n = 6$ *Stat1*$^{-/-}$ ilea with two panels representative of the range of signal detected shown. In **l**, *Stat1*$^{-/-}$ $n = 34$, 5 litters; *Stat1*$^{-/-}$*Cd300lf*$^{-/-}$ $n = 7$, 2 litters; and *Stat1*$^{-/-}$*Cd300lf*$^{-/-}$*Cd300ld*$^{-/-}$ $n = 19$, 3 litters; $^{**}P = 0.0066$, $^{****}P < 0.0001$. In **m**, *Stat1*$^{-/-}$ $n = 12$, 3 litters; *Stat1*$^{-/-}$*Cd300lf*$^{-/-}$ $n = 6$, 2 litters; and *Stat1*$^{-/-}$*Cd300lf*$^{-/-}$*Cd300ld*$^{-/-}$ $n = 6$, 2 litters; $^{**}P = 0.0019$ (*Stat1*$^{-/-}$ vs *Stat1*$^{-/-}$*Cd300lf*$^{-/-}$, ileum), $^{**}P = 0.0082$ (*Stat1*$^{-/-}$ vs *Stat1*$^{-/-}$*Cd300lf*$^{-/-}$*Cd300ld*$^{-/-}$, ileum), $^{**}P = 0.0069$ (*Stat1*$^{-/-}$ vs *Stat1*$^{-/-}$*Cd300lf*$^{-/-}$, colon), $^{***}P = 0.0002$ (*Stat1*$^{-/-}$ vs *Stat1*$^{-/-}$*Cd300lf*$^{-/-}$*Cd300ld*$^{-/-}$, colon), $^{***}P = 0.0002$ (*Stat1*$^{-/-}$ vs *Stat1*$^{-/-}$*Cd300lf*$^{-/-}$, spleen), $^{***}P = 0.0007$ (*Stat1*$^{-/-}$ vs *Stat1*$^{-/-}$*Cd300lf*$^{-/-}$*Cd300ld*$^{-/-}$, spleen), $^{**}P = 0.0014$ (*Stat1*$^{-/-}$ vs *Stat1*$^{-/-}$*Cd300lf*$^{-/-}$, brain), $^{***}P = 0.0002$ (*Stat1*$^{-/-}$ vs *Stat1*$^{-/-}$*Cd300lf*$^{-/-}$*Cd300ld*$^{-/-}$, brain). In **n**, *Stat1*$^{-/-}$ $n = 12$, 5 litters; *Stat1*$^{-/-}$*Cd300lf*$^{-/-}$ $n = 12$, 2 litters; and *Stat1*$^{-/-}$*Cd300lf*$^{-/-}$*Cd300ld*$^{-/-}$ $n = 9$, 2 litters. Dashed lines indicate limit of detection for assays.

https://doi.org/10.1038/s41564-023-01383-1

from infected dams only after P16 is consistent with the lack of coprophagic behaviour while pups rely exclusively on breastmilk. Indeed, cross-fostering pups of MNoV-infected dams to MNoV-naïve dams effectively eliminates litter infection[42]. If this natural transmission is bypassed by direct inoculation, however, distinct host factors in neonates promote viral RNA uptake but restrict productive infection.

Endocytosis in immature small intestinal enterocytes promotes early-life nutrient absorption, and early gut maturation delays growth and increases neonatal mortality[37,39,40]. Luminal material uptake also facilitates immune development, enabling passive immunity via transport of breastmilk antibodies, helping establish tolerance to food and microbial antigens[38]. However, our work demonstrates that pathogenic materials may also be taken up by endocytosis of luminal materials. Neonatal mice are highly susceptible to rotavirus until approximately P15–17, when gut closure occurs, and cortisone treatment of younger mice before inoculation decreases infection[43]. Thus, if permissive cells are available, passive uptake may facilitate neonatal infections. Conversely, early viral exposure induces innate and adaptive responses,

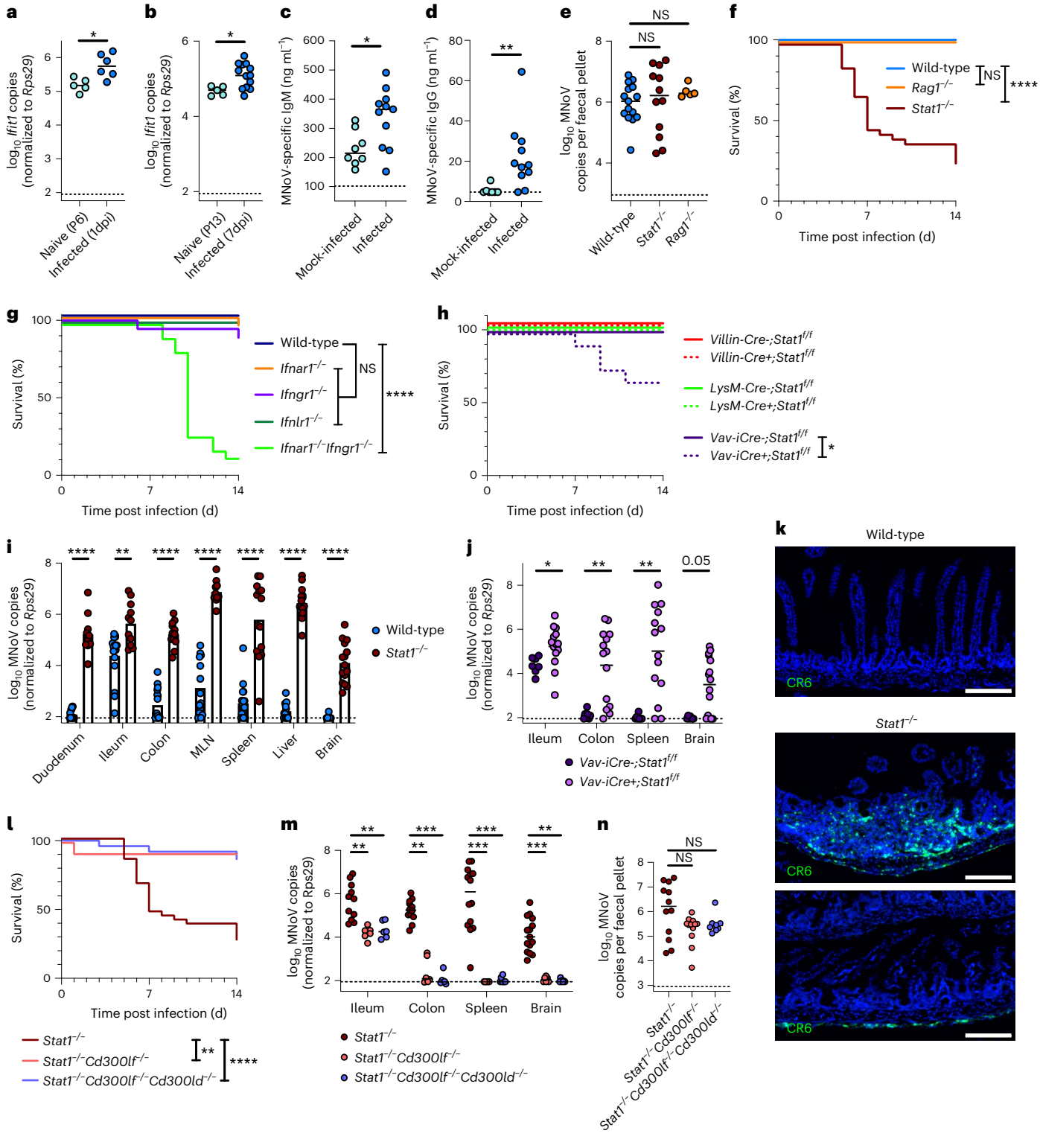

raising the possibility that non-specific endocytosis can protect against later infections. Juvenile mice represent an intriguing intermediate group, as they may experience non-specific endocytosis early in infection, but have undergone intestinal maturation by 7 dpi. Future studies exploring the long-term immunological impact of juvenile infection may reveal how exposures throughout development influence adult immunity.

The persistence of viral RNA after clearance of infectious virus is recognized for numerous RNA viruses including measles virus and SARS-CoV-2. RNA persistence may complicate diagnosis, as viral RNA can be detected after infectious virions have cleared. Persistent RNA may also contribute to chronic immune activation, although its consequences have not been well-defined and may be pathogen- and site-specific[35]. Heightened IEC shedding in neonates may contribute to prolonged detection of faecal CR6 RNA.

Additional barriers limit neonatal CR6 infection despite passive inoculum uptake. Tuft cells, the target of CR6 in adults, are undetectable in our neonatal mice. Non-epithelial cells also express CD300 molecules, although expression may vary between neonates and adults[44]. Our data support the idea that without viral restriction by IFNs in haematopoietic cells, CR6 replicates in non-tuft cells in neonates, leading to viral dissemination and lethality. CR6 infection is more lethal in *Stat1*$^{-/-}$ neonates versus *Stat1*$^{-/-}$ adults[31,32]. Viral sensors such as MDA5 and RIG-I are upregulated at weaning compared with early life[45], so *Stat1*-independent responses in adult mice may limit severe infection. Early-life endocytosis may also increase viral uptake compared with CD300LF-dependent infection alone. Alternatively, the microbiota enables CR6 infection in adult mice[24] and the neonatal gut microbiome composition is distinct from adults[46], so unique features of the neonatal *Stat1*$^{-/-}$ microbiota may increase infectivity.

Beyond increased lethality in *Stat1*$^{-/-}$ mice, the specific IFNs controlling CR6 are distinct in neonates versus adults. Type III IFNs control intestinal CR6 replication[15], while type I IFNs limit CR6 extraintestinal dissemination in adults[33]. In contrast, regulation of CR6-driven neonatal lethality is dominated by type I and II IFNs, although type III IFNs may also play a role. Involvement of different IFNs may reflect age-dependent tissue-specificity of IFN responses. In adults, IECs primarily express the type III IFN receptor[47], while neonatal IECs respond to both type I and III IFNs[48]. Multiple IFN classes may thus control viral replication and restrict systemic spread in neonates.

CD300LF plays a minor role in CR6 RNA uptake in wild-type neonates, as disrupting or blocking this receptor decreased viral RNA. Similarly, blocking virus replication with 2-CMC starting at 0 dpi reduced viral RNA shedding, whereas treatment at 3 dpi did not, suggesting early replication. Interestingly, CD300LF has been implicated in facilitating cellular internalization of MNoV not via direct capsid binding but instead via interactions with phosphatidylserines[49] while shuttling vesicle-cloaked viral clusters into the endocytic pathway[50]. We found that cortisone reduced viral RNA shedding in *Cd300lf*$^{-/-}$ but not in wild-type neonates. Thus, whether CD300LF itself could contribute to passive ileal absorption of virus in neonates remains an intriguing open question. CD300LF dependence is revealed in *Stat1*$^{-/-}$ neonates, as CD300LF is necessary for systemic spread[13]. Our work thus identifies numerous context-dependent host factors regulating viral RNA shedding in neonatal mice.

Despite children's high disease burden and important role in NoV transmission, host factors contributing to age-specific prolonged viral shedding are not well-defined. Host immunity limits NoV persistence, as immunocompromised patients of all ages experience extremely prolonged viral shedding[51]. Although anti-NoV antibodies accumulate with age, correlated with decreasing infection prevalence[52], antibody protection is limited in duration and against heterologous strains[3,53], and thus may not fully explain age-based differences. Innate immune regulation of NoV infection has not been well-studied in humans, although many aspects of innate immunity are immature in children[54]. Whether differences in immune control can explain the variation in disease progression in young children is thus currently unclear. Our study points to both physiological and innate immune characteristics regulating viral outcomes that differ between neonates and juvenile or adult mice, highlighting the critical need to explore how developmental changes may govern infection responses.

Methods

Mice

Unless otherwise specified, C57BL/6J wild-type mice were originally purchased from Jackson Laboratories (JAX 000664) and bred and housed in WUSTL animal facilities under specific-pathogen-free, including MNoV-free, conditions. Animal protocols were approved by the Washington University Institutional Animal Care and Use Committee (protocol numbers 20160126, 20190162 and 22-1040). Animals were housed at up to five adult mice in a cage or a single dam with a lactating litter. The conditions in animal rooms used in this study fall within the standards set by the 'Guide for the Care and Use of Laboratory Animals'. Temperatures were maintained between 68–72 °F and humidity between 30–70%. The room light cycle is 12 h light:12 h dark. Age- and sex-matched adults were used in adult mouse infections. Litters of pups including males and females were used in neonatal mouse experiments. No statistical methods were used to predetermine sample sizes, but our sample sizes are similar to those reported in previous publications[19].

Fig. 5 | Persistent MNoV replicates in neonates in the absence of STAT1 signalling. a–**c**, *Stat1*$^{-/-}$ pups were orally inoculated with CR6 at P6. 2-CMC (100 mg kg^{-1}) or PBS was injected subcutaneously daily to littermates beginning at 3 dpi and survival tracked through 7 dpi (**a**). Tissues were collected at 7 dpi (**b**) and stool collected at 1–7 dpi (**c**) and MNoV genome copies quantified by RT-qPCR. **d**,**e**, Wild-type pups were orally inoculated with CR6 at P6. 2-CMC (100 mg kg^{-1}) or PBS was injected subcutaneously daily to littermates beginning at 0 dpi or 3 dpi. Ilea (**d**) and stool (**e**) were collected at 7 dpi and MNoV genome copies quantified by RT-qPCR. **f**,**g**, Wild-type neonates (P6) and adults (6–9 weeks old) were orally inoculated with CR6. Infectious virus from 3–10 dpi stool (**f**) and 7 dpi tissues (**g**) was quantified by plaque assay on BV2 cells. **h**,**i**, *Stat1*$^{-/-}$ neonates were orally inoculated with CR6 at P6. Infectious virus from stool (**h**) and tissues (**i**) collected at 5–6 dpi was quantified by plaque assay on BV2 cells. **j**, *Stat1*$^{-/-}$ pups were orally inoculated with CR6 at P6. Spleen samples were collected at 5 dpi and stained for CD45, dsRNA and NS6/7. Scale bar, 30 µm. **k**, Wild-type neonates were orally inoculated with CR6 at P6 and faecal pellets collected from dam and pups at 14 dpi. MNoV genome copies were quantified by RT-qPCR and MNoV+ dams defined as those with MNoV genome copies above the limit of detection. **l**, *Cd300lf*$^{-/-}$ neonates were inoculated with CR6 at P6 and faecal pellets collected from dam and pups at 7, 10 and 14 dpi and MNoV genome copies quantified by RT-qPCR, with 7 dpi pup stool replicated from Fig. 3a. **m**, *Rps29* expression in stool samples from wild-type naïve and CR6-inoculated neonates (inoculated at P6, collected at P13, P20) or adult mice (naïve vs 14 dpi) was assessed by RT-qPCR. Data were analysed using Gehan-Breslow-Wilcoxon test (**a**), two-way ANOVA with Šídák's multiple comparisons (**d**,**e**), two-tailed Mann-Whitney test corrected with the Holm-Šídák method (**f**,**g**), two-tailed Mann-Whitney test (**k**) and two-way ANOVA with Tukey's multiple comparisons (**m**). In **a**–**c**, 2-CMC $n = 6$; PBS $n = 4$, from two litters; (**a**) $^{**}P = 0.0023$. In **d** and **e**, day 0 PBS $n = 6$; 2-CMC $n = 4$, from two litters; day 3 PBS $n = 6$; 2-CMC $n = 8$, from two litters. (**d**) $^{**}P = 0.0055$. (**e**) $^{**}P = 0.0051$. In **f**, P6 $n = 5$, 3 dpi; $n = 7$, 7 dpi; $n = 4$, 10 dpi; from two litters; and adult $n = 8$, 3 dpi; $n = 9$, 7 dpi; $n = 6$, 10 dpi; from two experiments; $^{**}P = 0.0047$ (3 dpi), $^{*}P = 0.0113$ (7 dpi, 10 dpi). In **g**, P6 $n = 6$, from two litters; and adult $n = 6$, from two experiments; $^{**}P = 0.0043$ (ileum and colon). In **h** and **i**, $n = 6$, from 2 litters. **j**, Representative of three independent samples, remaining replicates and controls in Extended Data Fig. 8. In **k**, MNoV+ pups $n = 21$, from 5 litters; MNoV− pups $n = 20$, from 5 litters; $^{****}P < 0.0001$. In **l**, $n = 20$, from 3 litters. In **m**, naïve pups $n = 12$, 2 litters; CR6 pups $n = 6$, 3 litters; naïve adults $n = 11$, 2 experiments; CR6-inoculated adults $n = 6$, 1 experiment; $^{*}P = 0.0285$, $^{**}P = 0.0073$, $^{***}P = 0.0004$. Dashed lines indicate limit of detection for assays.

https://doi.org/10.1038/s41564-023-01383-1

Knockout mice in the C57BL/6J background were maintained in the same conditions and included the following strains: *Pou2f3*$^{-/-}$[32], *Cd300lf*$^{-/-}$[12], *Rag1*$^{-/-}$ (JAX 002216)[55], *Stat1*$^{-/-}$ (JAX 012606)[56], *Ifnar1*$^{-/-}$[57], *Ifngr1*$^{-/-}$ (JAX 003288)[58] and *Ifnlr1*[14]. *Ifnar1*$^{-/-}$ mice were originally provided by Michael Aguet (ISREC - School of Life Sciences Ecole Polytechnique Fédérale de Lausanne). *Pou2f3*$^{-/-}$, *Cd300lf*$^{-/-}$, and *Ifnlr1*$^{-/-}$ mice were previously generated at Washington University in St. Louis. *Ifnar1*$^{-/-}$*Ifngr1*$^{-/-}$ mice were generated by crossing *Ifnar1*$^{-/-}$ and *Ifngr1*$^{-/-}$ mice.

Stat1 conditional knockout mice were generated by crossing *Stat1*$^{f/f}$ mice (MMRRC 32054)[59] to the following Cre lines: *Villin-Cre* (JAX 004586)[60], *Lysm-Cre* (JAX 004781)[61] and *Vav-iCre* (JAX 008610)[62,63].

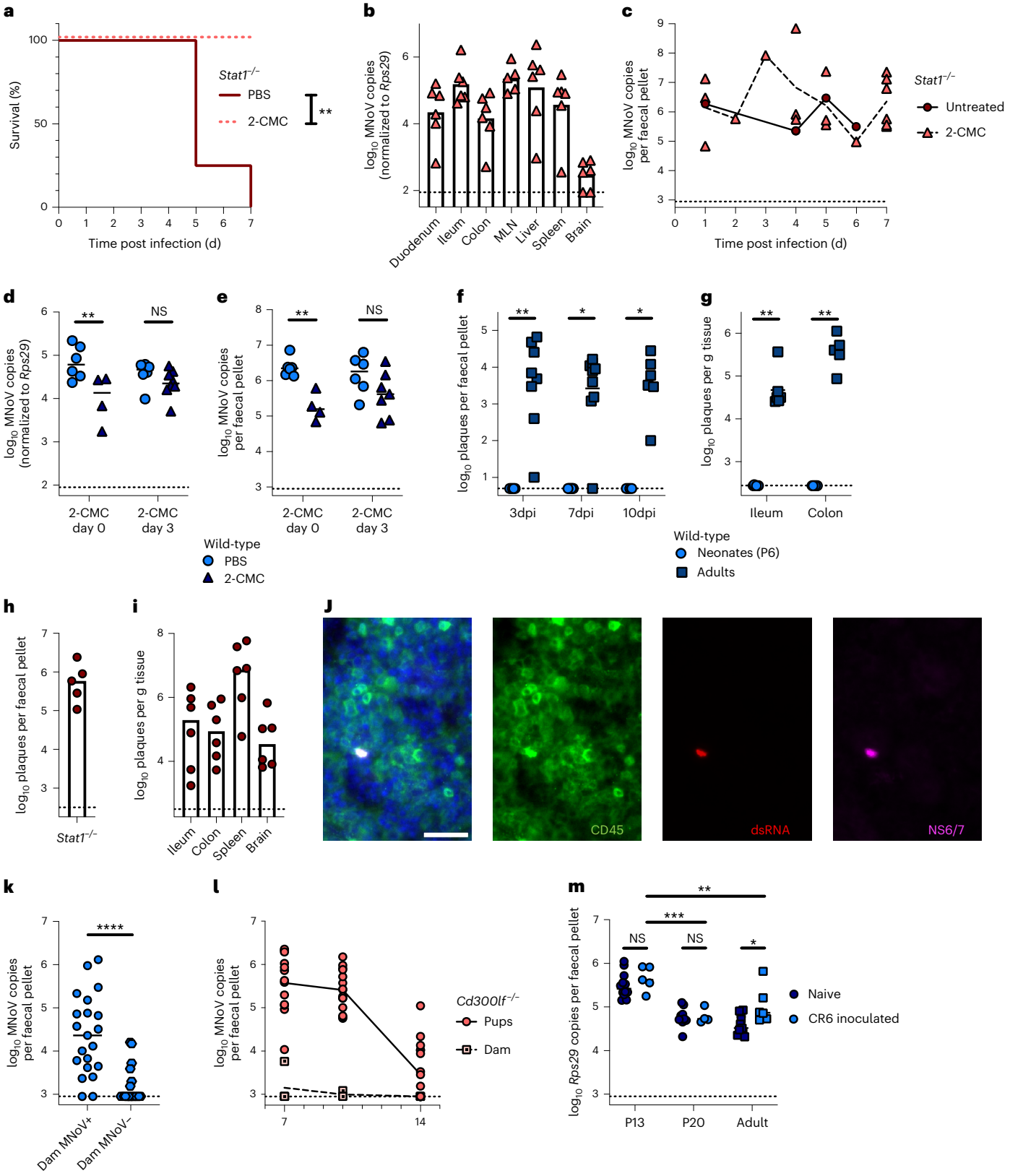

https://doi.org/10.1038/s41564-023-01383-1

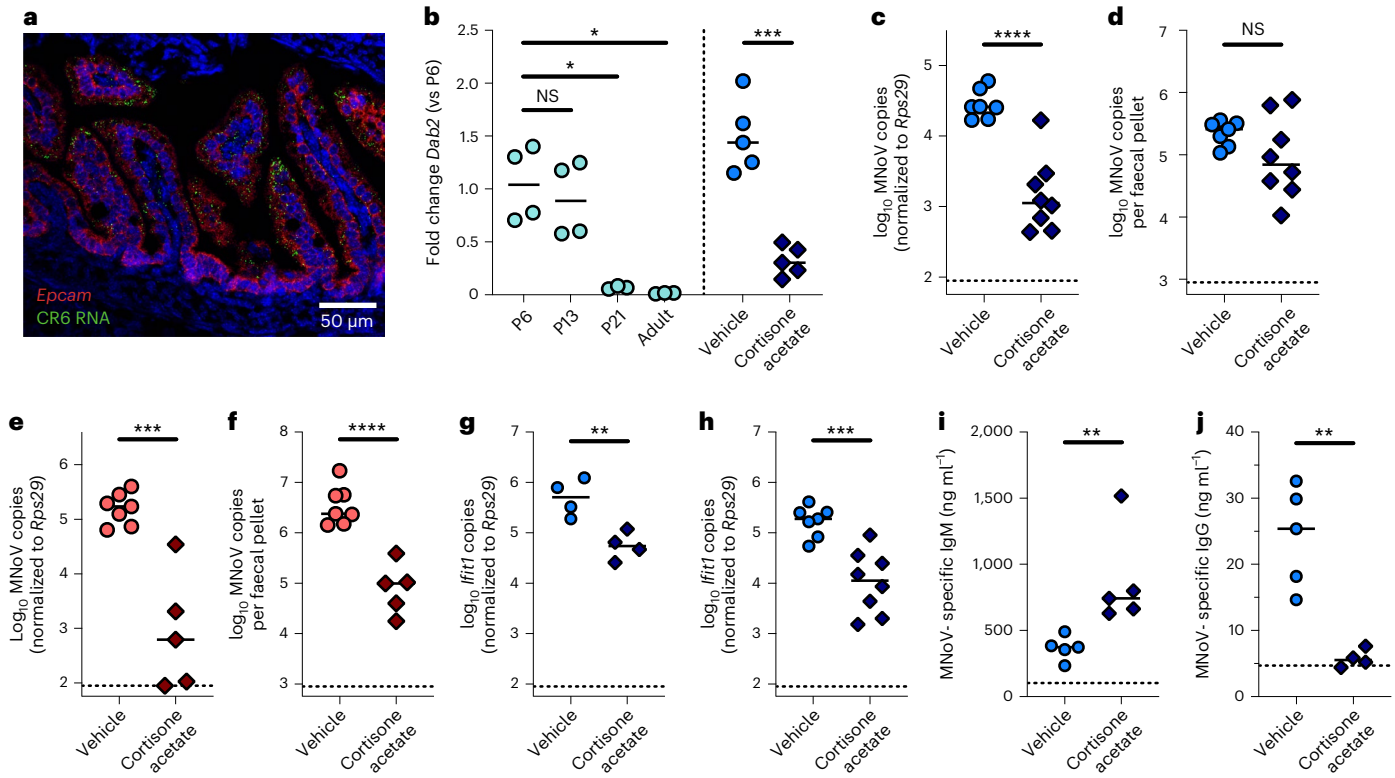

Fig. 6 | Non-specific uptake leads to the accumulation of persistent MNoV RNA in neonatal small intestines. a, Wild-type neonates were orally inoculated with CR6 at P6 and ilea collected at 8 hpi and stained for CR6 and *Epcam* RNA using RNA in situ hybridization. **b**, Ileal samples were collected from naïve mice at P6, P13, P21 and as adults (left) or at 7 dpi (P13) from littermates inoculated with CR6 and treated subcutaneously with 0.5 mg g^{-1} cortisone acetate or vehicle at P6 (right). *Dab2* expression was quantified by RT-qPCR. **c**,**d**, Wild-type littermates were orally inoculated with CR6 and injected subcutaneously with 0.5 mg g^{-1} cortisone acetate or vehicle at P6. Ilea (7 dpi; **c**) and stool (**d**) MNoV genome copies were quantified by RT-qPCR. **e**,**f**, *Cd300lf*$^{-/-}$ littermates were inoculated with CR6 and treated subcutaneously with 0.5 mg g^{-1} cortisone acetate or vehicle at P6. Ilea (7 dpi; **e**) and stool (**f**) MNoV genome copies were quantified by RT-qPCR. **g**–**j**, Wild-type neonates were orally inoculated with CR6 and treated subcutaneously with 0.5 mg g^{-1} cortisone acetate or vehicle at P6. *Ifit1* expression at 1 dpi (**g**) and 7 dpi (**h**) was quantified by RT-qPCR. Serum was collected at 14 dpi and anti-MNoV IgM (**i**) and IgG (**j**) were quantified by ELISA, with vehicle data overlapping with Fig. 4a–d. Data were analysed using Welch's ANOVA with Dunnett's multiple comparisons (**b**, time course), two-tailed *t*-test (**b**, vehicle vs cortisone acetate, **e**–**h**,**j**), Welch's two-tailed *t*-test (**c**,**d**) and two-tailed Mann-Whitney test (**i**). **a**, Representative sample; remaining replicates shown in Extended Data Fig. 8. In **b**, P6 $n = 4$, 1 litter; P13 $n = 4$, 2 litters; P21 $n = 3$, 2 litters; adult $n = 3$, 1 experiment; 7 dpi cortisone acetate $n = 5$, 2 litters; 7 dpi vehicle $n = 5$, 2 litters; $^{*}P = 0.0283$ (P6 vs P21), $^{*}P = 0.0243$ (P6 vs adult), $^{***}P = 0.0001$ (vehicle vs cortisone acetate). In **c** and **d**, cortisone acetate $n = 8$ or vehicle $n = 7$, from 3 litters; (**c**) $^{****}P < 0.0001$. In **e** and **f**, cortisone acetate $n = 5$ or vehicle $n = 7$, from 2 litters; (**e**) $^{***}P = 0.0003$, (**f**) $^{****}P < 0.0001$. In **g**, 2 independent litters (4 pups per group); $^{**}P = 0.0061$. In **h**, 3 independent litters (7–8 pups per group), analysed by two-tailed *t*-test; $^{***}P = 0.0004$. In **i** and **j**, 2 independent litters (5 pups per group); (**i**) $^{**}P = 0.0079$, (**j**) $^{**}P = 0.0022$. Dashed lines indicate limit of detection for assays.

All infections were performed on Cre+ and Cre− littermates born to Cre− dams. *Vav-iCre* pups were screened for germline deletion of the floxed allele.

Cd300lf$^{-/-}$*Cd300ld*$^{-/-}$ mice were generated by co-injecting guide RNAs targeting the *CD300lf* and *Cd300ld* loci into C57BL/6J fertilized zygotes along with Cas9 mRNA. A founder mouse with the following mutations was recovered:

Cd300lf locus – WT:CGATATACCTCA–GGCTGGAAGGAT
KO:CGATATACCTCAAGGCTGGAAGGAT
Cd300ld locus – WT:TATTCCTCATAC–TGGAAGGGTTAC
KO:TATTCCTCATACGTGGAAGGGTTAC

Additional generations were genotyped by Transnetyx from tail biopsy specimens using real-time PCR with mutation-specific probes.

For comparison of pups by vendor source (Extended Data Fig. 1A), C57BL/6 mice were bred at WUSTL, or purchased as lactating dams with litters from Jackson Laboratories (JAX 000664) or Charles River (CR 027). For comparison of pups by genetic background (Extended Data Fig. 1B), C57BL/6 (000664), BALB/c (000651), A/J (000646), NOD (001976) and 129S1 (002448) lactating dams with litters were purchased from JAX. PWK/PhJ (003715) adults were purchased from JAX and bred at WUSTL due to unavailability of lactating dams for this strain. For comparison of C57BL/6 and BALB/c pups (Extended Data Fig. 1C,D), lactating dams with litters were purchased from CR (CR 027 and 028, respectively). For comparison of C57BL/6 and BALB/c adults (Extended Data Figs. 1E,F), 6-week-old adults were purchased from CR (CR 027 and 028, respectively).

Generation of viral stocks

Stocks of MNoV strain CR6 were generated from molecular clones as previously described[13]. Briefly, plasmids encoding the viral genomes were transfected into 293T cells to generate infectious virus, which was subsequently passaged on BV2 cells. After two passages, BV2 cultures were frozen and thawed to liberate virions. Virus was concentrated by centrifugation in a 100,000 MWCO ultrafiltration unit (Vivaspin, Sartorius). Titres of virus stocks were determined by plaque assay on BV2 cells.

MNoV infections and sample collection

For adult MNoV infections, 6–9-week-old mice were orally inoculated with 1×10^6 plaque-forming units (p.f.u.) of CR6 in a volume of 25 µl. For

neonatal and juvenile infections, P6 and P15 mice, respectively, were gavaged with 1×10^6 p.f.u. of CR6 in a volume of 50 µl using a 22 gauge plastic feeding tube. Virus stocks contained a range of $1 \times 10^{7.4}$–$1 \times 10^{7.7}$ genome copies in 1×10^6 p.f.u. Stool samples were collected by gently palpating the abdomen to encourage defecation. Given the challenge of collecting stool from young mice, stool was collected as possible, and the number of samples collected was generally representative of a much greater number of mice. Tissues were collected from mice at the time of euthanasia or shortly after natural death when tissues were still intact. Stool and tissues were collected into 2 ml tubes (Sarstedt) with 1-mm-diameter zirconia/silica beads (Biospec). Samples were frozen and stored at −80 °C until RNA extraction or plaque assay. For controls for treatment groups, infected groups included mice treated with PBS or PBS containing 2% Tween-80.

RNA extraction and quantitative reverse transcription PCR (RT-qPCR)

As previously described[14], RNA was isolated from stool using a ZR-96 viral RNA kit (Zymo Research) according to the manufacturer's protocol. RNA from tissues was isolated using TRI reagent with a Direct-zol-96 RNA kit (Zymo Research) according to the manufacturer's protocol. RNA (5 µl) from stool or tissue was used for complementary DNA synthesis with the ImPromII reverse transcriptase system (Promega). MNoV *Taq*Man assays were performed using a standard curve for determination of absolute viral genome copies. PrimeTime RT-qPCR assays were used for *Cd300lf* (Mm.PT.58.13995989), *Ifit1* (Mm.PT.58.32674307) and *Mx2* (Mm.PT.58.11386814) using a standard curve. SYBR green PCR was performed for *Dab2* (Fw 5′-TCATCAAACCCCTCTGTGGT, Rv 5′-AGCGAGGACAGAGGTCAACA), *Naga* (Fw 5′- TGCCTTCCTAGCTGACTATGC, Rv 5′- GTCATTTTGCCCATGTCCTC), *Prdm1* (Fw 5′- AGTTCCCAAGAATGCCAACA, Rv 5′- TTTCTCCTCATTAAAGCCATCAA), *Sis* (Fw 5′- TGCCTGCTGTGGAAGAAGTAA, Rv 5′- CAGCCACGCTCTTCACATTT) using Power SYBR Green master mix (Applied Biosystems). RT-qPCR for housekeeping gene *Rps29* was performed as previously described[14]. All samples were analysed with technical duplicates.

MNoV-specific enzyme-linked immunosorbent assay (ELISA)

CR6 at a concentration of 5×10^6 p.f.u. per well diluted in PBS was used to coat a 96-well MaxiSorp plate overnight at 4 °C. Twofold serial dilutions in PBS of mouse IgG (Sigma-Aldrich, I5381, starting at 12.5 ng ml^{-1}) or mouse IgM (Sigma-Aldrich, PP50, starting at 250 ng ml^{-1}) were used to coat plates overnight as standard controls. Wells were washed three times with wash buffer (0.05% Tween-20 in PBS) between incubations. After 1 h of blocking with 1% BSA in PBS (blocking buffer), serum diluted in blocking buffer at 1:50 was incubated for 2 h. After washing, anti-mouse IgG-HRP (Sigma-Aldrich, A3673, 1:2,000 dilution in blocking buffer) or anti-mouse IgM-HRP (Sigma-Aldrich, A8786, 1:2,000 dilution in blocking buffer) was incubated for 2 h. After washing, ELISA TMB Substrate solution (eBioscience) was added and the reaction stopped with the addition of stop solution (2 N H_2SO_4). Optical density was read at 450 nm and reference wavelength 570 nm, and concentration of samples was determined against the standard curve.

RNA-ISH

Ilea and colons were collected, and intestinal contents flushed with 10% neutral buffered formalin. Tissues were Swiss rolled and fixed overnight in 10% neutral buffered formalin at 4 °C, washed three times with 70% ethanol and embedded in paraffin. RNAscope assays were performed using RNAscope Multiplex Fluorescent v2 assays (ACD) according to manufacturer instructions. Briefly, 5 µm sections were baked at 60 °C for 1 h, then deparaffinized by washing with xylene and 100% ethanol. Antigen retrieval was performed by boiling sections in Target Retrieval reagent (ACD) for 15 min, followed by 30 min of treatment with Protease Plus (ACD) at 40 °C. Tissues were hybridized with a custom-designed probe against MNoV strain CR6 RNA (ACD; 20 probe pairs targeted to strain CR6, within nucleotides 5359–6394 as in GenBank accession number JQ237823.1; used undiluted), and in some experiments a probe against *Epcam* (418151, ACD, diluted 1:50 in MNoV probe), for 2 h at 40 °C, followed by amplification and development of channel-specific signals according to manufacturer protocol, and staining with DAPI to visualize nuclei. Positive- and negative-control probes were included to validate staining protocols. Images were acquired using an AxioScan Z1 (Zeiss) slide scanner, and ImageJ (v.2.9.0) was used to analyse the images.

Immunofluorescent staining

Ilea and colon sections were Swiss rolled and paraffin embedded as described above. Staining for DCLK1 and NS6/7 was generally performed as described previously[10]. Briefly, 5 µm sections were deparaffinized by washing three times (5 min each) in xylene and isopropanol, followed by 5 min in running water and 5 min in Tris buffered saline with 0.1% Tween-20 (TBST). Antigen retrieval was performed by boiling for 10 min in antigen unmasking solution (Vector), followed by washing for 5 min in TBST. Blocking was performed in 1% bovine serum albumin and 10% goat serum in TBST for 30 min at room temperature. When staining for dsRNA, an additional 1 h blocking with F(ab) fragment anti-mouse IgG (ab6668, Abcam, 0.1 mg ml^{-1}) was performed. Primary staining was performed overnight at 4 °C using rabbit anti-DCLK1 (D2U3L, Cell Signaling, 62257S, 1:300), guinea pig anti-NS6/7 (1:1,000, gift from Kim Green) and mouse anti-dsRNA (rJ2, MilliporeSigma, MABE113425, 1:200). Samples were washed in TBST, followed by secondary staining for 1 h at room temperature with goat anti-rabbit AlexaFluor 488 (A11008, Invitrogen, 1:500), goat anti-guinea pig AlexaFluor 647 (A21450, Invitrogen, 1:500) and goat anti-mouse AlexaFluor 555 (A21425, Invitrogen, 1:500). Samples were washed in TBST, counterstained with DAPI (1:1,000) and mounted with Fluorshield mounting media. Tuft cells were quantified as DCLK1-positive cells per crypt/villus, counting at least 50 crypts/villi per mouse, beginning at the distal end of the ileum and the proximal end of the colon.

Plaque assay

For CR6 plaque assays, BV2 cells were seeded at 2×10^6 cells per well in a 6-well plate and grown overnight. Tissues were weighed and samples homogenized by bead beating in 500 µl DMEM medium. Samples were spun at 2,500 *g* for 3 min at 4 °C, then the supernatant was removed and incubated for 1 h at room temperature with rocking. Tenfold dilutions were prepared and applied to each well of BV2 cells, followed by 1 h of incubation at room temperature with gentle rocking. Inoculum was removed and 2 ml of overlay media was added (MEM, 10% FBS, 2 mM L-glutamine, 10 mM HEPES and 1% methylcellulose). Plates were incubated for 72 h before visualization after crystal violet staining (0.2% crystal violet and 20% ethanol).

Fc-CD300lf blocking

CR6 neutralization was assessed in vitro by measuring cytotoxicity. BV2 cells (2×10^4 per well) were plated in a 96-well plate. CR6 was incubated with dilutions of the Fc region of murine IgG2b fused to the human CD300LF ectodomain[13] or mouse CD300LF ectodomain[30] for 1 h at 37 °C and used to infect BV2 cells at a multiplicity of infection of 0.05. Plates were incubated at 37 °C for 48 h, then 25 µl of CellTiter Glo (Promega, G7571) added per well and luminescence measured using a BioTek Synergy 2 plate reader with an integration time of 1 second to quantify viability via cellular ATP concentrations. Assays were performed in triplicate.

For neutralization with Fc-fusion proteins in vivo, 1×10^6 p.f.u. CR6 was incubated with 1.17 µg of human or mouse Fc-CD300lf in 50 µl media for 1 h at 37 °C before oral infection as described above.

Mouse treatments

Cortisone acetate (Sigma, C3130) was dissolved to 25 mg ml^{-1} in PBS containing 2% Tween-80 at 37 °C and vortexed to make a fine

suspension before injection. Mice were treated by subcutaneous injection at 0.5 mg g^{-1} body weight[41] or the equivalent volume of vehicle using a 31 ga (neonates) or 28 ga (adults) needle to inject into the scruff. Cortisone acetate reduced weight gain and variably contributed to death in pups, probably due to reduced nutrient absorption after premature gut maturation.

2-CMC (Neta Scientific, AST-F12743) was dissolved to 20 mg ml^{-1} in PBS. Mice were treated by subcutaneous injection at 100 mg kg^{-1} body weight[34] or the equivalent volume of vehicle using a 31 ga needle to inject into the scruff daily.

For intestinal transit time assessment, mice were gavaged with 50 µl (neonates) or 400 µl (adults) of a 1% Evans blue solution. Faecal pellets were resuspended in PBS and intestines were collected from neonatal mice for assessment of blue colour.

Statistical analysis

Data were analysed using GraphPad Prism 9 software. In all graphs, NS indicates not significant ($P > 0.05$), *$P < 0.05$, **$P < 0.01$, ***$P < 0.001$ and ****$P < 0.0001$. Data were tested for normal distribution using Shapiro-Wilk tests and non-parametric tests were performed if data were not normally distributed. *F* tests or Brown Forsythe tests were performed to confirm equal variances between groups. No statistical method was used to predetermine sample size. No data were excluded from the analyses. When possible, littermate controls were randomized to groups to minimize weight variability between groups. The investigators were not blinded to allocation during experiments and outcome assessment, except for tuft cell quantification which was performed blinded to sample source.

Reporting summary

Further information on research design is available in the Nature Portfolio Reporting Summary linked to this article.

Materials availability

All reagents are available from M.T.B. under a material transfer agreement with Washington University.

Data availability

Data from this study are included in the main paper and in Extended Data. Source data are provided with this paper.

References

1. Grytdal, S. P. et al. Incidence of norovirus and other viral pathogens that cause acute gastroenteritis (AGE) among Kaiser Permanente member populations in the United States, 2012–2013. *PLoS ONE* **11**, e0148395 (2016).
2. Cannon, J. L., Lopman, B. A., Payne, D. C. & Vinjé, J. Birth cohort studies assessing norovirus infection and immunity in young children: a review. *Clin. Infect. Dis.* **69**, 357–365 (2019).
3. Saito, M. et al. Multiple norovirus infections in a birth cohort in a Peruvian periurban community. *Clin. Infect. Dis.* **58**, 483–491 (2014).
4. Shioda, K. et al. Can use of viral load improve norovirus clinical diagnosis and disease attribution? *Open Forum Infect. Dis.* **4**, ofx131 (2017).
5. Simmons, K., Gambhir, M., Leon, J. & Lopman, B. Duration of immunity to norovirus gastroenteritis. *Emerg. Infect. Dis.* **19**, 1260–1267 (2013).
6. Baldridge, M. T., Turula, H. & Wobus, C. E. Norovirus regulation by host and microbe. *Trends Mol. Med.* **22**, 1047–1059 (2016).
7. Grau, K. R. et al. The major targets of acute norovirus infection are immune cells in the gut-associated lymphoid tissue. *Nat. Microbiol.* **2**, 1586–1591 (2017).
8. Graziano, V. R. et al. CD300lf conditional knockout mouse reveals strain-specific cellular tropism of murine norovirus. *J. Virol.* **95**, e01652–20 (2020).
9. Nice, T. J., Strong, D. W., McCune, B. T., Pohl, C. S. & Virgin, H. W. A single-amino-acid change in murine norovirus NS1/2 is sufficient for colonic tropism and persistence. *J. Virol.* **87**, 327–334 (2013).
10. Wilen, C. B. et al. Tropism for tuft cells determines immune promotion of norovirus pathogenesis. *Science* **360**, 204–208 (2018).
11. Haga, K. et al. Functional receptor molecules CD300lf and CD300ld within the CD300 family enable murine noroviruses to infect cells. *Proc. Natl Acad. Sci. USA* **113**, E6248–E6255 (2016).
12. Orchard, R. C. et al. Discovery of a proteinaceous cellular receptor for a norovirus. *Science* **353**, 933–936 (2016).
13. Graziano, V. R. et al. CD300lf is the primary physiologic receptor of murine norovirus but not human norovirus. *PLoS Pathog.* **16**, e1008242 (2020).
14. Baldridge, M. T. et al. Expression of Ifnlr1 on intestinal epithelial cells is critical to the antiviral effects of interferon lambda against norovirus and reovirus. *J. Virol.* **91**, e02079-16 (2017).
15. Nice, T. J. et al. Interferon-λ cures persistent murine norovirus infection in the absence of adaptive immunity. *Science* **347**, 269–273 (2015).
16. Nice, T. J. et al. Type I interferon receptor deficiency in dendritic cells facilitates systemic murine norovirus persistence despite enhanced adaptive immunity. *PLoS Pathog.* **12**, e1005684 (2016).
17. Grau, K. R. et al. The intestinal regionalization of acute norovirus infection is regulated by the microbiota via bile acid-mediated priming of type III interferon. *Nat. Microbiol.* **5**, 84–92 (2020).
18. Thackray, L. B. et al. Critical role for interferon regulatory factor 3 (IRF-3) and IRF-7 in type I interferon-mediated control of murine norovirus replication. *J. Virol.* **86**, 13515–13523 (2012).
19. Roth, A. N. et al. Norovirus infection causes acute self-resolving diarrhea in wild-type neonatal mice. *Nat. Commun.* **11**, 2968 (2020).
20. Helm, E. W. et al. Environmentally-triggered contraction of the norovirus virion determines diarrheagenic potential. *Front. Immunol.* **13**, 1043746 (2022).
21. Ebino, K. Y. Studies on coprophagy in experimental animals. *Jikken Dobutsu* **42**, 1–9 (1993).
22. Rasmussen, T. S. et al. Mouse vendor influence on the bacterial and viral gut composition exceeds the effect of diet. *Viruses* **11**, 435 (2019).
23. Hildebrand, F. et al. Inflammation-associated enterotypes, host genotype, cage and inter-individual effects drive gut microbiota variation in common laboratory mice. *Genome Biol.* **14**, R4 (2013).
24. Baldridge, M. T. et al. Commensal microbes and interferon-λ determine persistence of enteric murine norovirus infection. *Science* **347**, 266–269 (2015).
25. Blutt, S. E., Warfield, K. L., O'Neal, C. M., Estes, M. K. & Conner, M. E. Host, viral, and vaccine factors that determine protective efficacy induced by rotavirus and virus-like particles (VLPs). *Vaccine* **24**, 1170–1179 (2006).
26. Gerbe, F. et al. Intestinal epithelial tuft cells initiate type 2 mucosal immunity to helminth parasites. *Nature* **529**, 226–230 (2016).
27. Saqui-Salces, M. et al. Gastric tuft cells express DCLK1 and are expanded in hyperplasia. *Histochem. Cell Biol.* **136**, 191–204 (2011).
28. Schneider, C. et al. A metabolite-triggered tuft cell-ILC2 circuit drives small intestinal remodeling. *Cell* **174**, 271–284.e14 (2018).
29. Haber, A. L. et al. A single-cell survey of the small intestinal epithelium. *Nature* **551**, 333–339 (2017).
30. Nelson, C. A. et al. Structural basis for murine norovirus engagement of bile acids and the CD300lf receptor. *Proc. Natl Acad. Sci. USA* **115**, E9201–E9210 (2018).

31. Strong, D. W., Thackray, L. B., Smith, T. J. & Virgin, H. W. Protruding domain of capsid protein is necessary and sufficient to determine murine norovirus replication and pathogenesis in vivo. *J. Virol.* **86**, 2950–2958 (2012).
32. Walker, F. C. et al. Norovirus evolution in immunodeficient mice reveals potentiated pathogenicity via a single nucleotide change in the viral capsid. *PLoS Pathog.* **17**, e1009402 (2021).
33. Hwang, S. et al. Nondegradative role of Atg5-Atg12/Atg16L1 autophagy protein complex in antiviral activity of interferon gamma. *Cell Host Microbe* **11**, 397–409 (2012).
34. Rocha-Pereira, J., Van Dycke, J. & Neyts, J. Treatment with a nucleoside polymerase inhibitor reduces shedding of murine norovirus in stool to undetectable levels without emergence of drug-resistant variants. *Antimicrob. Agents Chemother.* **60**, 1907–1911 (2015).
35. Griffin, D. E. Why does viral RNA sometimes persist after recovery from acute infections? *PLoS Biol.* **20**, e3001687 (2022).
36. Zhang, Z. et al. IL-22-induced cell extrusion and IL-18-induced cell death prevent and cure rotavirus infection. *Sci. Immunol.* **5**, eabd2876 (2020).
37. Park, J. et al. Lysosome-rich enterocytes mediate protein absorption in the vertebrate gut. *Dev. Cell* **51**, 7–20.e6 (2019).
38. Weström, B., Arévalo Sureda, E., Pierzynowska, K., Pierzynowski, S. G. & Pérez-Cano, F.-J. The immature gut barrier and its importance in establishing immunity in newborn mammals. *Front. Immunol.* **11**, 1153 (2020).
39. Harper, J., Mould, A., Andrews, R. M., Bikoff, E. K. & Robertson, E. J. The transcriptional repressor Blimp1/Prdm1 regulates postnatal reprogramming of intestinal enterocytes. *Proc. Natl Acad. Sci. USA* **108**, 10585–10590 (2011).
40. Muncan, V. et al. Blimp1 regulates the transition of neonatal to adult intestinal epithelium. *Nat. Commun.* **2**, 452 (2011).
41. Daniels, V. G., Hardy, R. N., Malinowska, K. W. & Nathanielsz, P. W. The influence of exogenous steroids on macromolecule uptake by the small intestine of the new-born rat. *J. Physiol.* **229**, 681–695 (1973).
42. Compton, S. R. Prevention of murine norovirus infection in neonatal mice by fostering. *J. Am. Assoc. Lab. Anim. Sci.* **47**, 25–30 (2008).
43. Wolf, J. L., Cukor, G., Blacklow, N. R., Dambrauskas, R. & Trier, J. S. Susceptibility of mice to rotavirus infection: effects of age and administration of corticosteroids. *Infect. Immun.* **33**, 565–574 (1981).
44. Zenarruzabeitia, O. et al. The expression and function of human CD300 receptors on blood circulating mononuclear cells are distinct in neonates and adults. *Sci. Rep.* **6**, 32693 (2016).
45. Pott, J. et al. Age-dependent TLR3 expression of the intestinal epithelium contributes to rotavirus susceptibility. *PLoS Pathog.* **8**, e1002670 (2012).
46. Al Nabhani, Z. et al. A weaning reaction to microbiota is required for resistance to immunopathologies in the adult. *Immunity* **50**, 1276–1288.e5 (2019).
47. Sommereyns, C., Paul, S., Staeheli, P. & Michiels, T. IFN-lambda (IFN-λ) is expressed in a tissue-dependent fashion and primarily acts on epithelial cells in vivo. *PLoS Pathog.* **4**, e1000017 (2008).
48. Lin, J.-D. et al. Distinct roles of type I and type III interferons in intestinal immunity to homologous and heterologous rotavirus infections. *PLoS Pathog.* **12**, e1005600 (2016).
49. Voss, O. H., Tian, L., Murakami, Y., Coligan, J. E. & Krzewski, K. Emerging role of CD300 receptors in regulating myeloid cell efferocytosis. *Mol. Cell. Oncol.* **2**, e964625 (2015).
50. Santiana, M. et al. Vesicle-cloaked virus clusters are optimal units for inter-organismal viral transmission. *Cell Host Microbe* **24**, 208–220.e8 (2018).
51. Henke-Gendo, C. et al. New real-time PCR detects prolonged norovirus excretion in highly immunosuppressed patients and children. *J. Clin. Microbiol.* **47**, 2855–2862 (2009).
52. Nurminen, K. et al. Prevalence of norovirus GII-4 antibodies in Finnish children. *J. Med. Virol.* **83**, 525–531 (2011).
53. Newman, K. L. & Leon, J. S. Norovirus immunology: of mice and mechanisms. *Eur. J. Immunol.* **45**, 2742–2757 (2015).
54. Simon, A. K., Hollander, G. A. & McMichael, A. Evolution of the immune system in humans from infancy to old age. *Proc. Biol. Sci.* **282**, 20143085 (2015).
55. Mombaerts, P. et al. RAG-1-deficient mice have no mature B and T lymphocytes. *Cell* **68**, 869–877 (1992).
56. Durbin, J. E., Hackenmiller, R., Simon, M. C. & Levy, D. E. Targeted disruption of the mouse Stat1 gene results in compromised innate immunity to viral disease. *Cell* **84**, 443–450 (1996).
57. Muller, U. et al. Functional role of type I and type II interferons in antiviral defense. *Science* **264**, 1918–1921 (1994).
58. Huang, S. et al. Immune response in mice that lack the interferon-gamma receptor. *Science* **259**, 1742–1745 (1993).
59. Wallner, B. et al. Generation of mice with a conditional Stat1 null allele. *Transgenic Res.* **21**, 217–224 (2012).
60. Madison, B. B. et al. *Cis* elements of the villin gene control expression in restricted domains of the vertical (crypt) and horizontal (duodenum, cecum) axes of the intestine. *J. Biol. Chem.* **277**, 33275–33283 (2002).
61. Clausen, B. E., Burkhardt, C., Reith, W., Renkawitz, R. & Förster, I. Conditional gene targeting in macrophages and granulocytes using LysMcre mice. *Transgenic Res.* **8**, 265–277 (1999).
62. Ogilvy, S. et al. Promoter elements of vav drive transgene expression in vivo throughout the hematopoietic compartment. *Blood* **94**, 1855–1863 (1999).
63. Shimshek, D. R. et al. Codon-improved Cre recombinase (iCre) expression in the mouse. *Genesis* **32**, 19–26 (2002).

Acknowledgements

We thank all members of the Baldridge laboratory for helpful discussions, and specifically H. Deng and L. Foster for assistance with mouse colony maintenance; and R. Orchard (University of Texas Southwestern Medical Center) for providing Fc-CD300lf complexes. We are grateful to Kim Green (NIAID, NIH) for providing anti-NS6/7 antibody. We are grateful to Michael Aguet (ISREC - School of Life Sciences Ecole Polytechnique Fédérale de Lausanne) for providing *Ifnar1*$^{-/-}$ mice. This work was supported by the National Institutes of Health (NIH) grants R01AI141478 (S.M.K., M.T.B.), R01AI139314 and R01AI127552 (M.T.B.), R01A1148467 (C.B.W.) and F31AI167499-01 (E.A.K.), as well as the Burroughs Wellcome Fund (C.B.W.), National Science Foundation DGE-1745038/DGE-2139839 (E.A.K.), and the Pew Biomedical Scholars Program of the Pew Charitable Trusts (M.T.B.). The funders had no role in study design, data collection and analysis, decision to publish or preparation of the manuscript.

Author contributions

E.A.K., A.D. and S.A. performed the experiments. E.A.K. and M.T.B. analysed the results. E.A.K., S.M.K., C.B.W. and M.T.B. designed the project. E.A.K. and M.T.B. wrote the manuscript. All authors read and edited the manuscript.

Competing interests

The authors declare no competing interests.

Additional information

Extended data is available for this paper at https://doi.org/10.1038/s41564-023-01383-1.

Supplementary information The online version contains supplementary material available at https://doi.org/10.1038/s41564-023-01383-1.

Correspondence and requests for materials should be addressed to Megan T. Baldridge.

Peer review information *Nature Microbiology* thanks Nihal Altan-Bonnet, Jason Mackenzie and the other, anonymous, reviewer(s) for their contribution to the peer review of this work.

https://doi.org/10.1038/s41564-023-01383-1

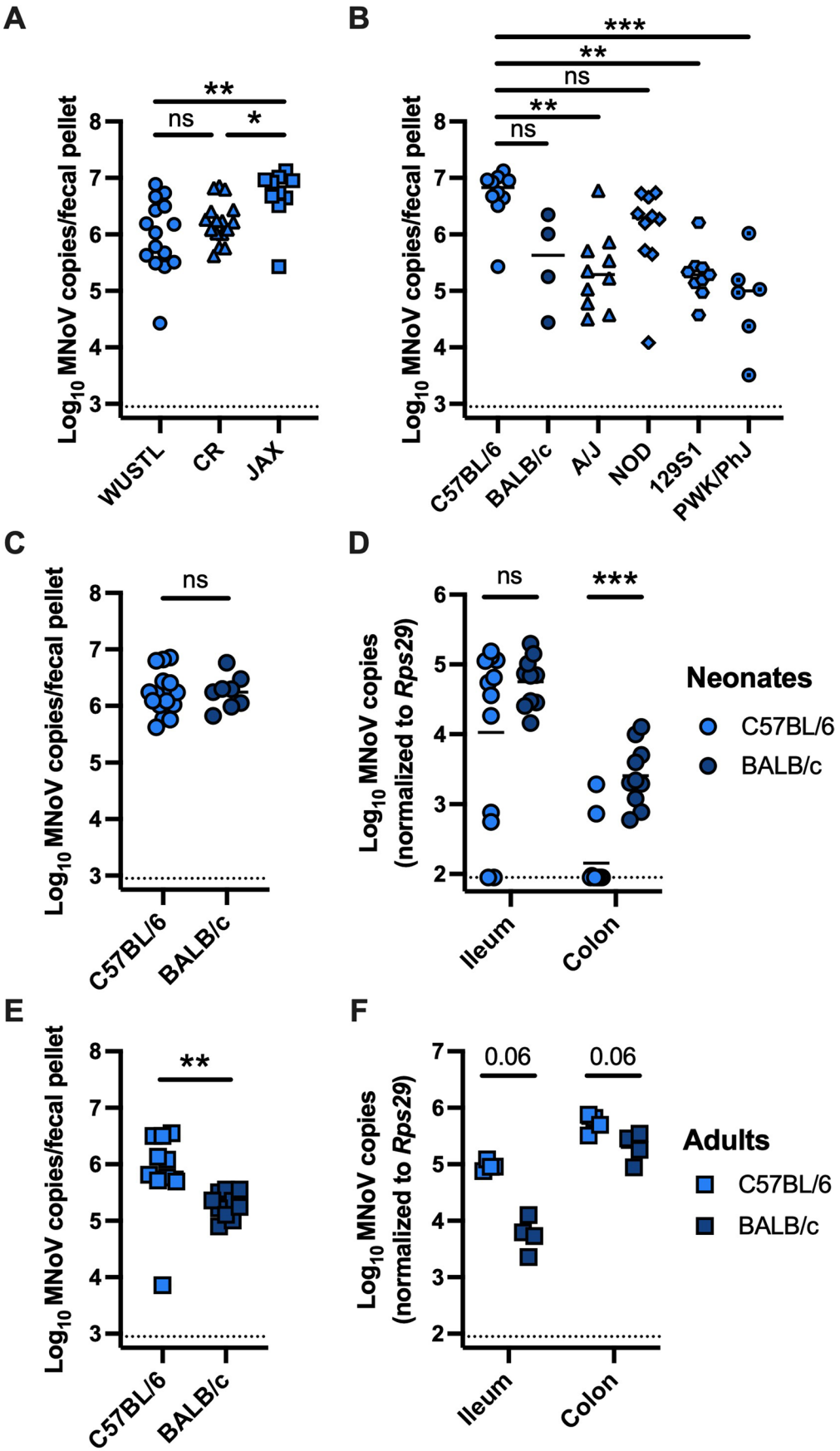

Extended Data Fig. 1 | See next page for caption.

https://doi.org/10.1038/s41564-023-01383-1

Extended Data Fig. 1 | Source and genetic background of mice influences persistent MNoV shedding as neonates and adults. (A) C57BL/6 neonates bred at Washington University in St. Louis (WUSTL), Charles River (CR), or Jackson Laboratories (JAX) were orally inoculated with CR6 at P6 and MNoV genome copies detected in 7dpi stool samples by RT-qPCR. **(B)** Neonates on the indicated backgrounds, all sourced from JAX, were orally inoculated with CR6 at P6 and MNoV genome copies detected in 7dpi stool samples by RT-qPCR. **(C, D)** Neonates on the indicated background, sourced from CR, were orally inoculated with CR6 at P6 and MNoV genome copies detected in 7dpi samples by RT-qPCR in stool **(C)** and tissues **(D)**. **(E, F)** Adult mice on the indicated background, sourced from CR, were orally inoculated with CR6 and MNoV genome copies detected in 10dpi samples by RT-qPCR in stool **(E)** and tissues **(F)**. Analyzed by Kruskal-Wallis test with Dunn's multiple comparisons test **(A, B)**, two-tailed t-test **(C)** two-tailed Mann-Whitney test **(D-F)** corrected with the Holm-Šídák method **(D, F)**. **(A)** WUSTL (n = 15, 4 litters), CR (n = 16, 3 litters), JAX (n = 10, 2 litters), *p = 0.0427, **p = 0.0037. **(B)** C57Bl/6 (n = 10, 2 litters), BALB/c (n = 4, 2 litters), A/J (n = 10, 3 litters), NOD (n = 10, 3 litters), 129S1 (n = 9, 2 litters), PWK/PhJ (n = 6, 2 litters), **p = 0.0023 (C57BL/6 vs. A/J), **p = 0.0012 (C57BL/6 vs. 129S1), ***p = 0.0003. **(C)** C57Bl/6 (n = 16, 3 litters), BALB/c (n = 8, 2 litters). **(D)** C57Bl/6 (n = 12, 2 litters), BALB/c (n = 10, 2 litters). ***p = 0.0001. **(E)** N = 10 mice per group from 2 independent experiments, **p = 0.0015. **(F)** N = 4 mice per group from one experiment, p = 0.0563 (ileum), p = 0.0571 (colon). Dashed lines indicate limit of detection for assays. ns, not significant (p > 0.05).

https://doi.org/10.1038/s41564-023-01383-1

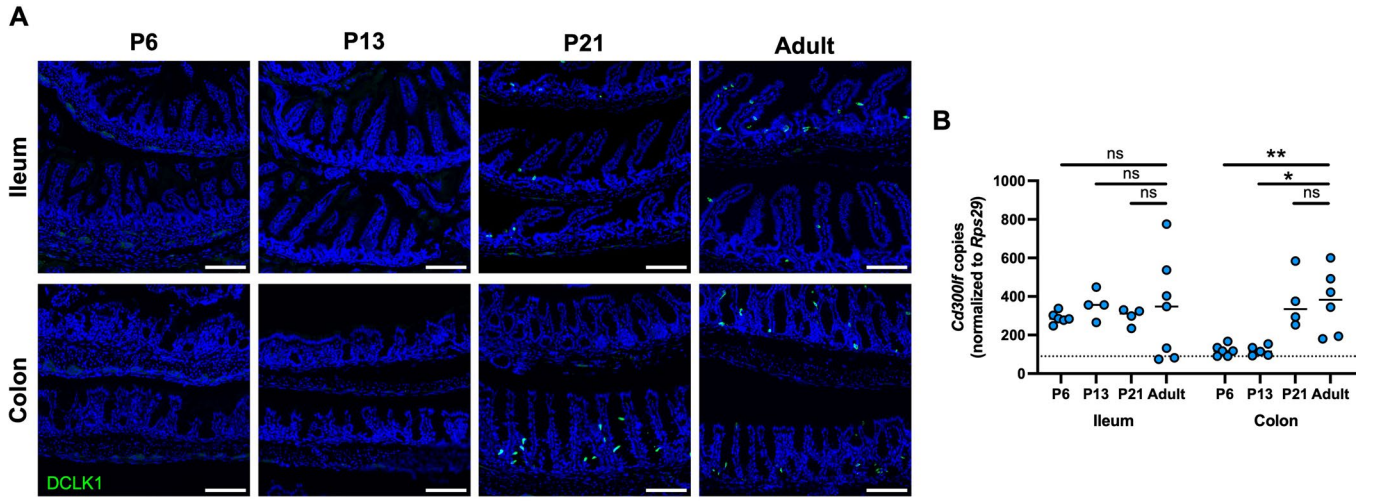

Extended Data Fig. 2 | Tuft cells and *Cd300lf* expression in early life. (A) Representative images of tuft cells quantified by immunofluorescent staining of DCLK1 in naïve C57BL/6 mice (quantified data shown in Fig. 3C). **(B)** *Cd300lf* was quantified in intestinal samples from naïve C57BL/6 mice by RT-qPCR at the indicated timepoints. P6 (n = 6, 1 litter), P13 (n = 4, 2 litters), P21 (n = 4, 2 litters), adult (n = 7, 2 experiments), analyzed by Kruskal-Wallis test with Dunn's multiple comparisons test. *p = 0.0183, **p = 0.0087. Dashed lines indicate limit of detection for assay. ns, not significant (p > 0.05).

https://doi.org/10.1038/s41564-023-01383-1

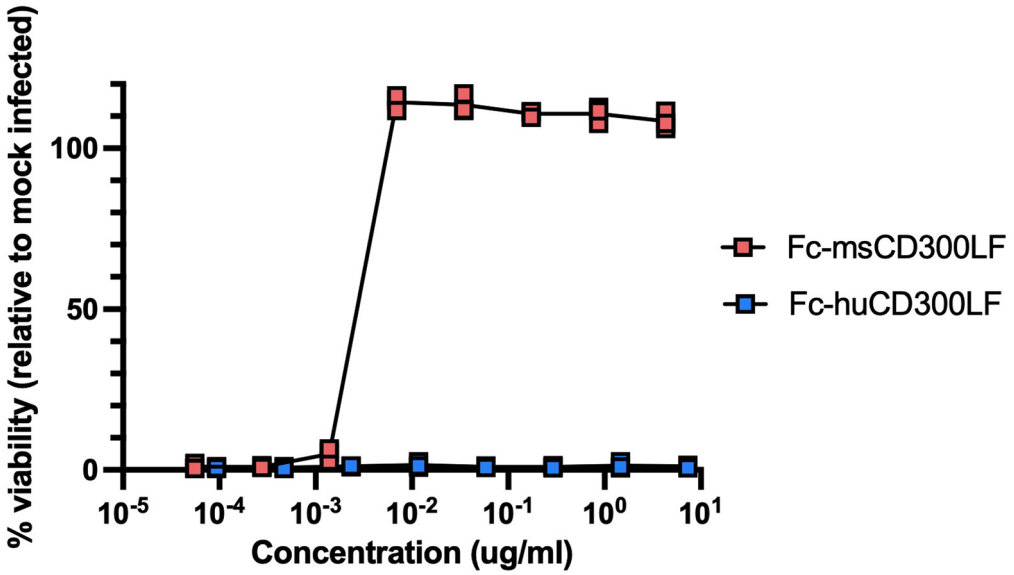

Extended Data Fig. 3 | Mouse but not human Fc-CD300LF blocks CR6 infection in vitro. CR6 was incubated with Fc-fusion proteins with either the human or mouse CD300LF ectodomains for 1 hour at 37 C, prior to infection of BV2 cells at an MOI of 0.05. Cell viability was measured by CellTiter Glo 48 hours post-infection. 3 technical replicates from a single experiment.

https://doi.org/10.1038/s41564-023-01383-1

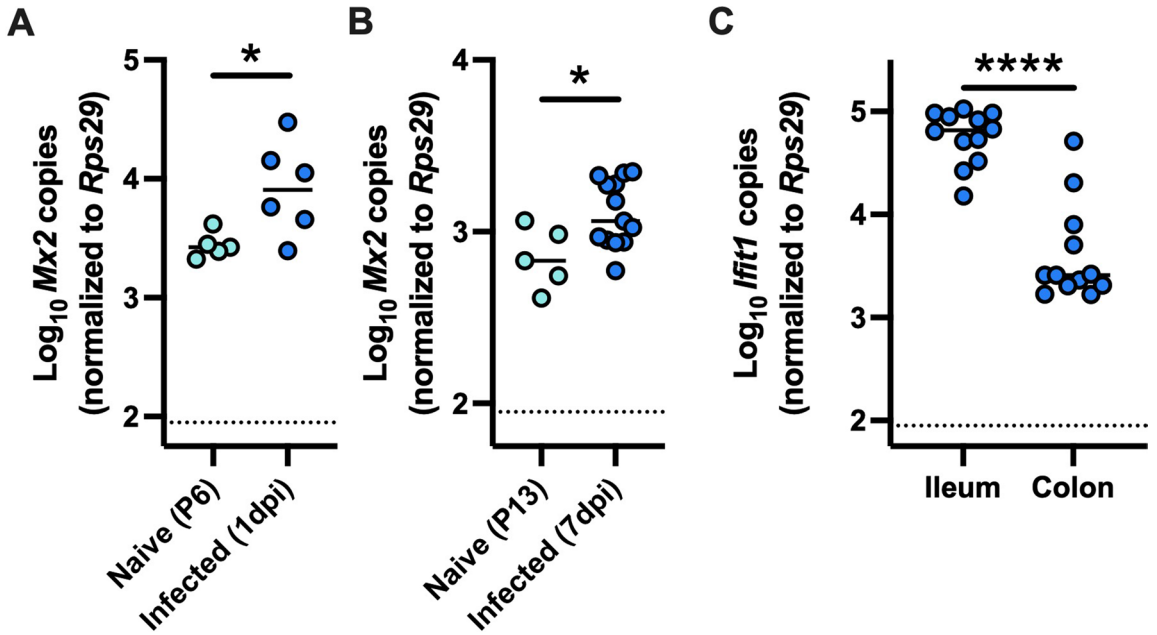

Extended Data Fig. 4 | CR6 induces ISG expression in the ileum. Wild-type neonates were orally inoculated with CR6 at P6. *Mx2* was quantified by RT-qPCR from ilea collected at 1 dpi **(A)** or 7 dpi **(B)** and compared to naïve neonates. **(C)** *Ifit1* expression was quantified in the ileum and colon of CR6-inoculated neonates at 7dpi. **(A)** Naïve (n = 5, 1 litter), infected (n = 6, 3 litters), analyzed by Welch's two-tailed t-test, *p = 0.0289. **(B)** Naïve (n = 5, 2 litters), infected (n = 13, 4 litters), analyzed by two-tailed t-test, **p = 0.0188. **(C)** N = 12 pups from 2 litters sourced from Charles River, analyzed by two-tailed Mann-Whitney test, ****p < 0.0001.

https://doi.org/10.1038/s41564-023-01383-1

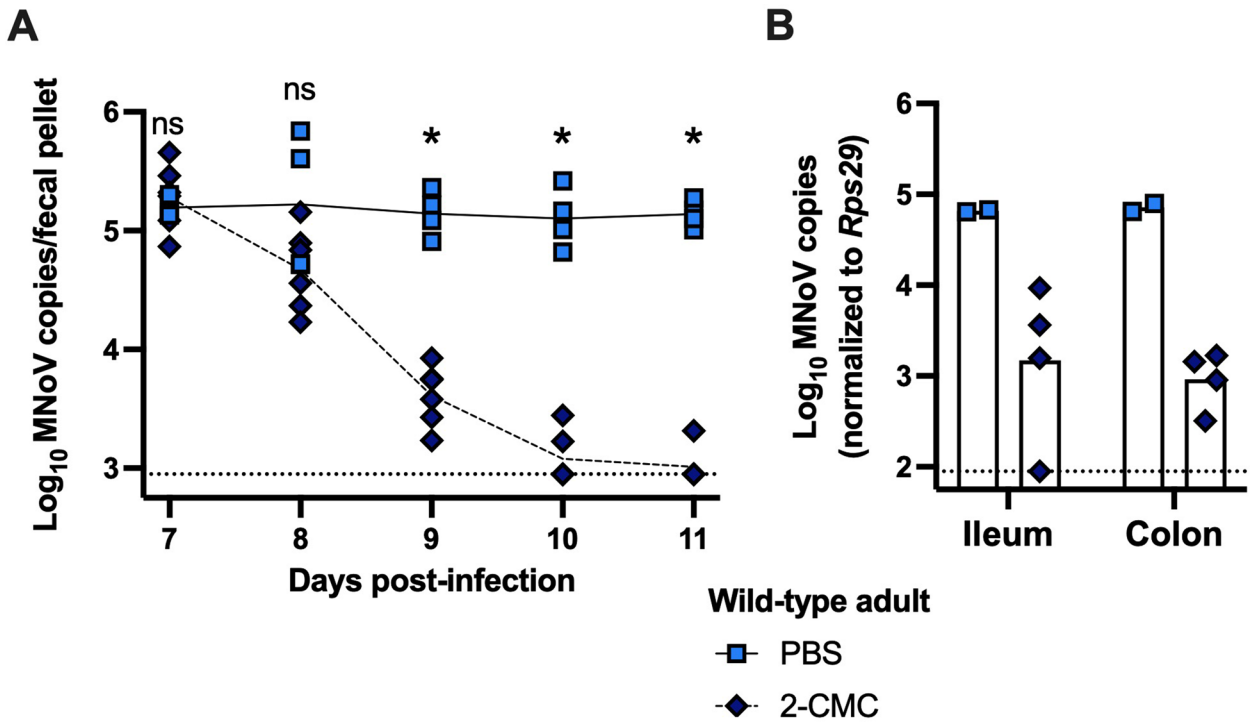

Extended Data Fig. 5 | 2-CMC blocks CR6 shedding in wild-type adult mice. Wild-type adult mice were orally inoculated with CR6. 100 mg/kg 2-CMC or PBS were injected subcutaneously daily at 7-9dpi. Stool was collected from 7-11dpi **(A)** and tissues at 11dpi **(B)**, and MNoV genome copies quantified by RT-qPCR. **(A)** PBS (n = 4), 2-CMC (n = 6), from two experiments. Analyzed by two-tailed Mann-Whitney test corrected with the Holm-Šídák method, *p = 0.0376 (9dpi, 10dpi), *p = 0.0236 (11dpi). **(B)** PBS (n = 2), 2-CMC (n = 4), from one experiment. Dashed lines indicate limit of detection for assays. ns, not significant.

https://doi.org/10.1038/s41564-023-01383-1

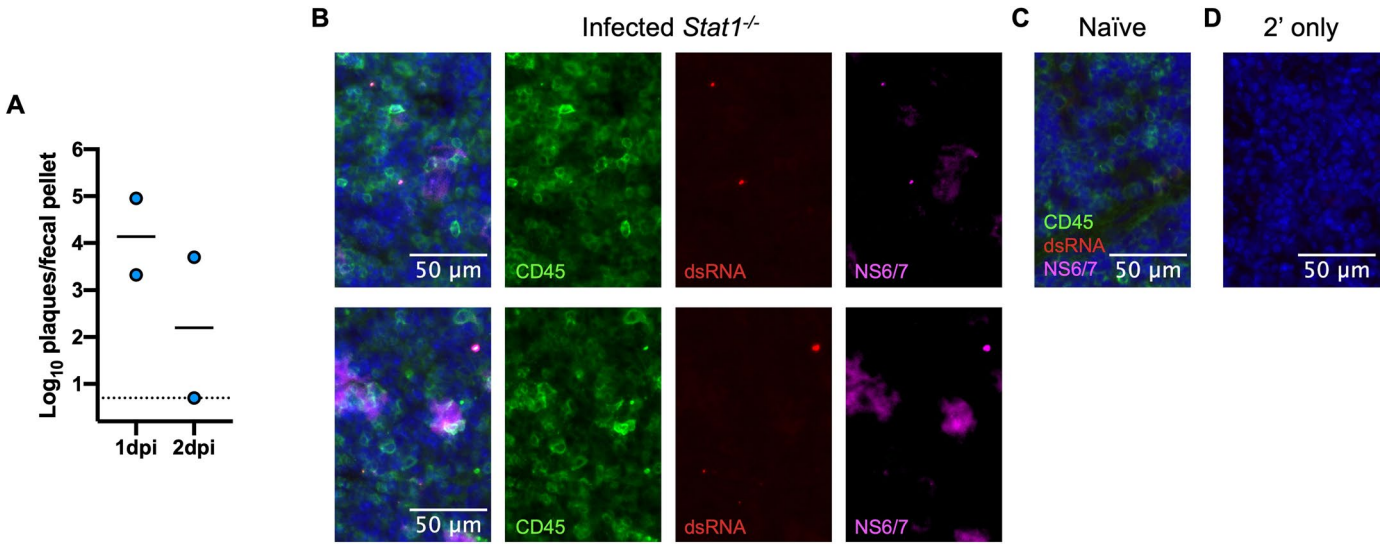

Extended Data Fig. 6 | CR6 replicates in the spleens of *Stat1*$^{-/-}$ neonates. (A) Wild-type neonates (P6) were orally inoculated with CR6. Infectious virus from 1-2dpi stool was quantified by plaque assay on BV2 cells. n = 2 stools collected per time point. **(B)** Additional replicates of spleens from CR6-inoculated *Stat1*$^{-/-}$ neonates, stained as in Fig. 5J. **(C)** Spleen from a naïve neonate stained as in Fig. 5J. **(D)** 2' only antibody control for spleen in Fig. 5J.

https://doi.org/10.1038/s41564-023-01383-1

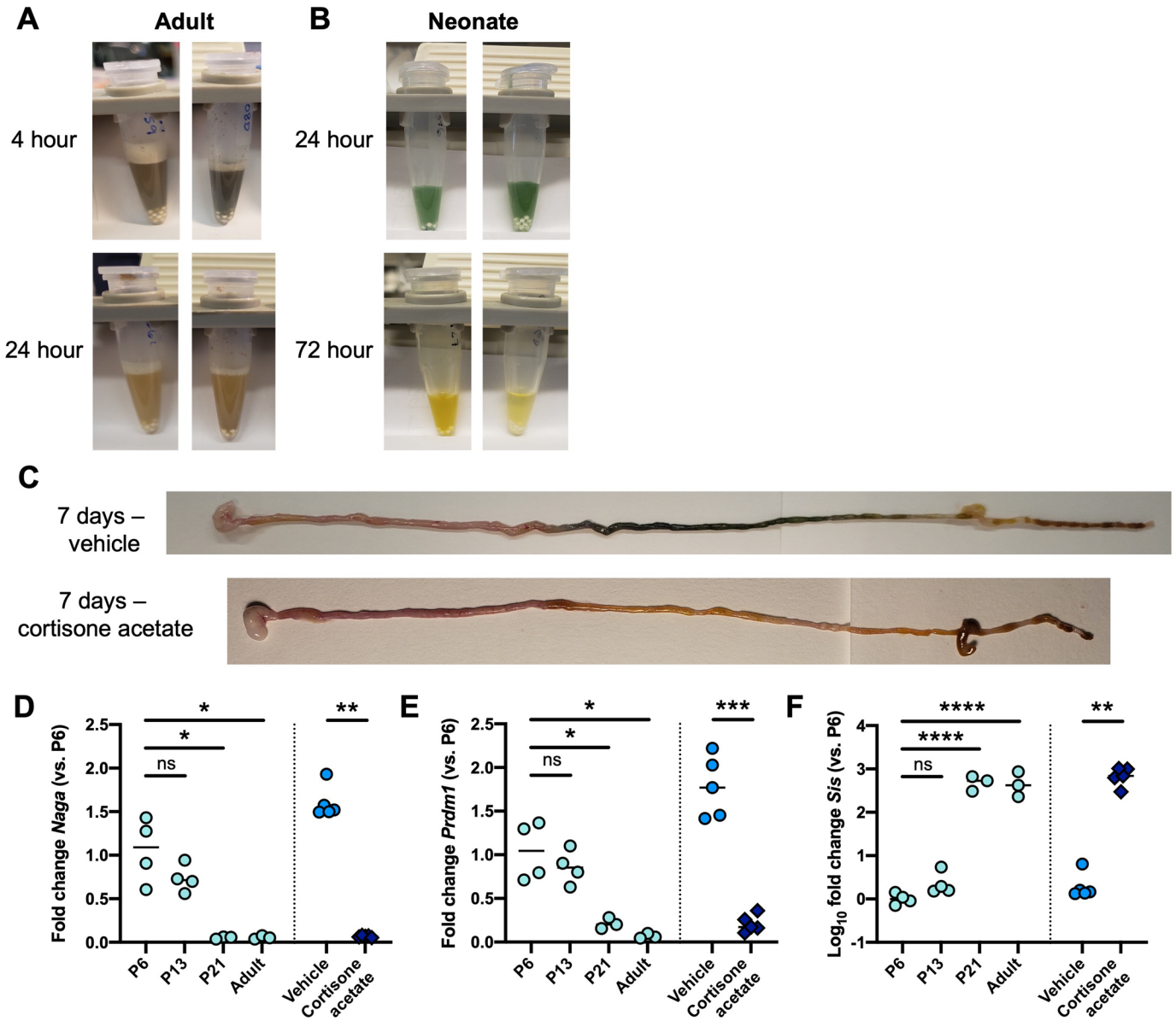

Extended Data Fig. 7 | Evans blue dye is retained in the distal small intestine of neonatal mice. (A) Adult mice were gavaged with 400ul Evans blue dye and stool collected at 4- and 24-hours post-gavage. **(B)** Neonates were gavaged at P6 with 50ul Evans blue dye and stool collected at 24- and 72-hours post-gavage. Stool was resuspended in PBS for assessment of blue colour. Representative of 3 adults from one experiment and 8 neonates from three litters. **(C)** Neonates were gavaged at P6 with 50ul Evans blue dye and treated with 0.5 mg/g cortisone acetate or vehicle. Intestines were collected at 7dpi post-gavage and assessed for blue colour across the length of the intestines. Representative of 3 cortisone acetate and 3 vehicle-treated neonates from two litters. **(D-F)** Ileal samples were collected from naïve mice at P6, P13, P21, and as adults (left) or at 7dpi (P13) from littermates inoculated with CR6 and treated subcutaneously with 0.5 mg/g cortisone acetate or vehicle at P6 (right). *Naga* **(D)**, *Prdm1* **(E)**, and *Sis* **(F)** expression was quantified by RT-qPCR. P6 (n = 4,1. litter), P13 (n = 4, 2 litters), P21 (n = 3, 2 litters), adult (n = 3, 1 experiment), 7dpi cortisone acetate (n = 5, 2 litters), 7dpi vehicle (n = 5, 2 litters). Naïve time course analyzed by Welch's ANOVA test with Dunnett's T3 multiple comparisons test **(D, E**, time course), ANOVA with Dunnett's multiple comparisons test **(F**, time course**)**, two-tailed Mann-Whitney test **(D, F**, vehicle vs. cortisone acetate**)**, or Welch's two-tailed t-test **(E**, vehicle vs cortisone acetate**)**. **(D)** *p = 0.0295 (P6 vs. P21), *p = 0.0298 (P6 vs. adult), **p = 0.0079 (vehicle vs. cortisone acetate). **(E)** *p = 0.0399 (P6 vs. P21), *p = 0.0245 (P6 vs. adult), ***p = 0.0003 (vehicle vs. cortisone acetate). **(F)** ****p < 0.0001 (P6 vs. P21, P6 vs. adult), **p = 0.0079 (vehicle vs. cortisone acetate). ns, not significant (p > 0.05).

https://doi.org/10.1038/s41564-023-01383-1

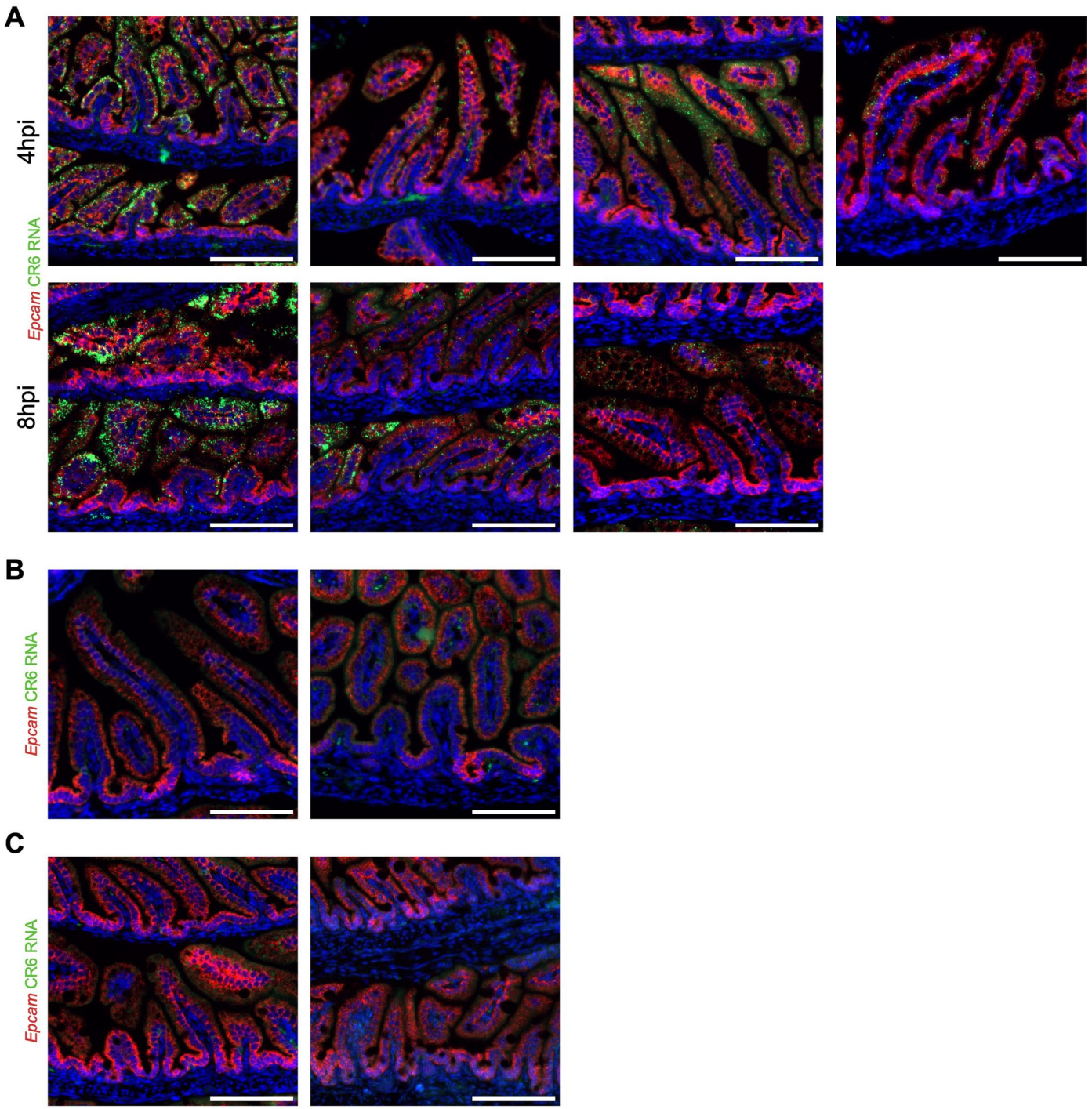

Extended Data Fig. 8 | CR6 uptake is localized to the distal small intestine. Ilea stained for *Epcam* and CR6 RNA. All replicates collected are shown. (**A**) Additional replicates of distal small intestinal sections from neonates inoculated with CR6 at P6, collected at 4 or 8hpi. (**B**) Proximal small intestinal sections collected at 8hpi. (**C**) Distal small intestinal sections from naïve neonates. Scale bars are 100μm long.

https://doi.org/10.1038/s41564-023-01383-1

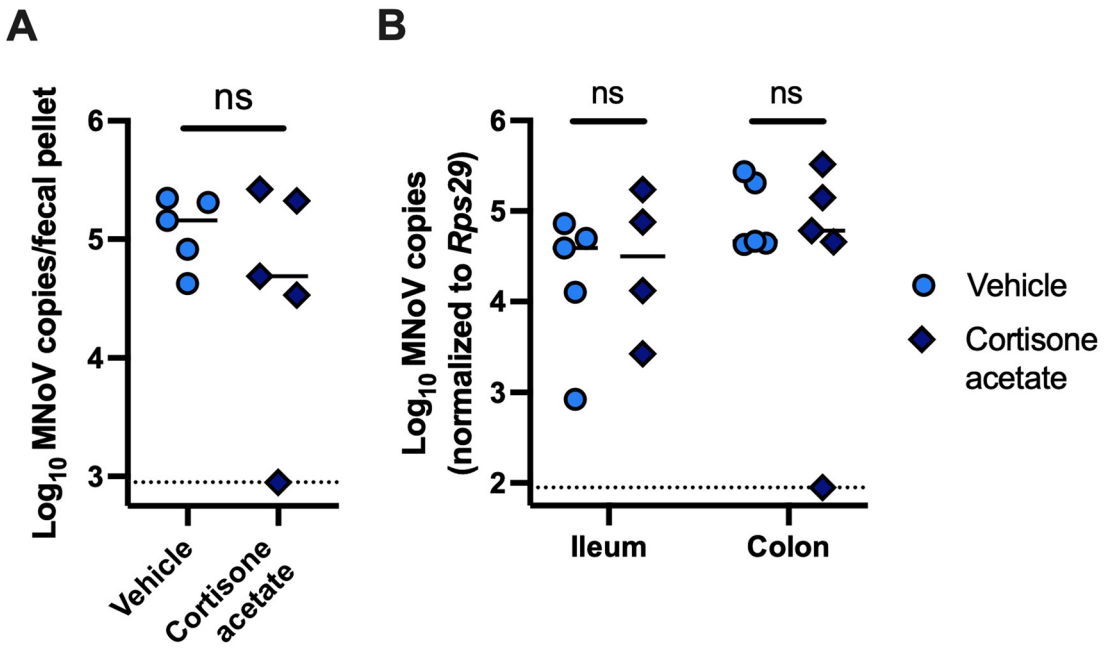

Extended Data Fig. 9 | Cortisone acetate treatment does not affect CR6 infection in adult mice. Wild-type adult mice were orally inoculated with CR6 and treated subcutaneously with 0.5 mg/g cortisone acetate or vehicle. Stool **(A)** and tissue **(B)** virus levels were quantified by RT-qPCR at 7dpi. Vehicle (n = 5) and cortisone acetate (n = 5), from two independent experiments. Analyzed by Welch's two-tailed t-test **(A)** and two-tailed Mann-Whitney test corrected with the Holm-Šídák method **(B)**. Dashed lines indicate limit of detection for assays. ns, not significant.

nature portfolio

Corresponding author(s): Baldridge, Megan

Last updated by author(s): Jun 29, 2022

Reporting Summary

Nature Portfolio wishes to improve the reproducibility of the work that we publish. This form provides structure for consistency and transparency in reporting. For further information on Nature Portfolio policies, see our Editorial Policies and the Editorial Policy Checklist.

Statistics

For all statistical analyses, confirm that the following items are present in the figure legend, table legend, main text, or Methods section.

n/a	Confirmed	
☐	☒	The exact sample size (*n*) for each experimental group/condition, given as a discrete number and unit of measurement
☐	☒	A statement on whether measurements were taken from distinct samples or whether the same sample was measured repeatedly
☐	☒	The statistical test(s) used AND whether they are one- or two-sided *Only common tests should be described solely by name; describe more complex techniques in the Methods section.*
☒	☐	A description of all covariates tested
☐	☒	A description of any assumptions or corrections, such as tests of normality and adjustment for multiple comparisons
☐	☒	A full description of the statistical parameters including central tendency (e.g. means) or other basic estimates (e.g. regression coefficient) AND variation (e.g. standard deviation) or associated estimates of uncertainty (e.g. confidence intervals)
☐	☒	For null hypothesis testing, the test statistic (e.g. *F*, *t*, *r*) with confidence intervals, effect sizes, degrees of freedom and *P* value noted *Give P values as exact values whenever suitable.*
☒	☐	For Bayesian analysis, information on the choice of priors and Markov chain Monte Carlo settings
☒	☐	For hierarchical and complex designs, identification of the appropriate level for tests and full reporting of outcomes
☒	☐	Estimates of effect sizes (e.g. Cohen's *d*, Pearson's *r*), indicating how they were calculated

Our web collection on statistics for biologists contains articles on many of the points above.

Software and code

Policy information about availability of computer code

Data collection	No software was used to collect data.
Data analysis	GraphPad Prism Version 9.0.2 was used for all statistical analyses. ImageJ (Version 2.9.0) was used to analyze microscopy images.

For manuscripts utilizing custom algorithms or software that are central to the research but not yet described in published literature, software must be made available to editors and reviewers. We strongly encourage code deposition in a community repository (e.g. GitHub). See the Nature Portfolio guidelines for submitting code & software for further information.

Data

Policy information about availability of data

All manuscripts must include a data availability statement. This statement should provide the following information, where applicable:

- Accession codes, unique identifiers, or web links for publicly available datasets
- A description of any restrictions on data availability
- For clinical datasets or third party data, please ensure that the statement adheres to our policy

The data from this study are tabulated in the main paper and supplementary materials. Data is uploaded as source data files. All reagents are available from M.T.B. under a material transfer agreement with Washington University.

Human research participants

Policy information about studies involving human research participants and Sex and Gender in Research.

Reporting on sex and gender	The study did not include human research participants.
Population characteristics	N/A
Recruitment	N/A
Ethics oversight	N/A

Note that full information on the approval of the study protocol must also be provided in the manuscript.

Field-specific reporting

Please select the one below that is the best fit for your research. If you are not sure, read the appropriate sections before making your selection.

☒ Life sciences ☐ Behavioural & social sciences ☐ Ecological, evolutionary & environmental sciences

For a reference copy of the document with all sections, see nature.com/documents/nr-reporting-summary-flat.pdf

Life sciences study design

All studies must disclose on these points even when the disclosure is negative.

Sample size	Sample size was chosen to identify phenotypes and reproduce results. Sample size was selected considering the Reduction principle in the 3R to use the minimum number of animals required to scientifically and statistically support the findings.
Data exclusions	No data were excluded from the analysis.
Replication	We state the number of experimental replicates in each figure legend. For visual analyses, we selected representative images and stated the number of time the experiment was repeated.
Randomization	When possible, littermates were used and treatment and control mice were randomly selected from the same cages to minimize weight variability between groups. For adult studies, sex- and age-matched controls were used and randomly assigned to treatment or control groups
Blinding	Tuft cell quantification was performed with blinding to groups. Otherwise, blinding was not used in our study as it does not have any clinical data or field sample collection

Reporting for specific materials, systems and methods

We require information from authors about some types of materials, experimental systems and methods used in many studies. Here, indicate whether each material, system or method listed is relevant to your study. If you are not sure if a list item applies to your research, read the appropriate section before selecting a response.

Materials & experimental systems

n/a	Involved in the study
☐	☒ Antibodies
☐	☒ Eukaryotic cell lines
☒	☐ Palaeontology and archaeology
☐	☒ Animals and other organisms
☒	☐ Clinical data
☒	☐ Dual use research of concern

Methods

n/a	Involved in the study
☒	☐ ChIP-seq
☒	☐ Flow cytometry
☒	☐ MRI-based neuroimaging

Antibodies

Antibodies used	rabbit anti-DCLK1 (D2U3L, Cell Signaling catalog #62257S, 1:300) Guinea pig anti-NS6/7 polyclonal antibody (provided by Kim Green, N/A, 1:1000) mouse anti-dsRNA (rJ2, MilliporeSigma, catalog #MABE113425, 1:200)

goat anti-rabbit AlexaFluor 488 (Invitrogen, catalog #A11008, 1:500)
goat anti-guinea pig AlexaFluor 647 (Invitrogen, catalog #A21450, 1:500)
goat anti-mouse AlexaFluor 555 (Invitrogen, catalog #A21425, 1:500).
mouse IgG (Sigma-Aldrich, catalog #I5381, starting at 12.5ng/ml)
mouse IgM (Sigma-Aldrich, catalog #PP50, starting at 250ng/ml)
anti-mouse IgG-HRP (Sigma-Aldrich, catalog #A3673, 1:2000)
anti-mouse IgM-HRP (Sigma-Aldrich, catalog #A8786, 1:2000)

Validation

Both anti-DCLK1 and anti-NS6/7 have been previously demonstrated to stain for the desired antigens (PMID: 29650672; PMID 28966054). Mouse anti-dsRNA have been used previously to detect single-stranded positive-sense virus in FFPE sections (PMID: 20729142). Minimal background staining was observed with DCLK1 in mice lacking tuft cells (Pou2f3-/-) and for NS6/7 and rJ2 in uninfected mice.

Mouse IgM and IgG and anti-mouse antibodies have been used widely for ELISAs (PMID: 32251490).

Eukaryotic cell lines

Policy information about cell lines and Sex and Gender in Research

Cell line source(s)

BV2 microglia cells were derived from female mice. 293T and BV2 cells were provided by Herbert "Skip" Virgin (Washington University in St. Louis).

Authentication

BV2 cells have been previously karyotyped (Clinical Genomics Research Unit, Washington University) by the GTW-banding method and determined to be hypertriploid (karyotype: 59~66,XX,-X/Y,-2,i(2)(A1),+3,-4,-6,add(8)(A1)x2,-9,-10,add(14)(A1),+15,+16,-17,-19,+6-10mar[cp10]). Aliquots of low passage cells are kept in liquid nitrogen storage and passage number is recorded.

293T cells were not authenticated.

Mycoplasma contamination

BV2 and 293T cells have been screened for mycoplasma.

Commonly misidentified lines
(See ICLAC register)

These cell lines are not commonly misidentified.

Animals and other research organisms

Policy information about studies involving animals; ARRIVE guidelines recommended for reporting animal research, and Sex and Gender in Research

Laboratory animals

C57BL/6J, Pou2f3-/-, Cd300lf-/-, Rag1-/- (B6.129S7-Rag1tm1Mom/J), Stat1-/- (B6.129S(Cg)-Stat1tm1Dlv/J), Ifnar1-/-, Ifngr1-/- (B6.129S7-Ifngr1tm1Agt/J), Ifnlr1-/-, Ifnar1-/-Ifngr1-/-, Stat1-fl (B6;129S-Stat1tm1Mam/Mmjax), Villin-Cre (B6.Cg-Tg(Vil1-cre)997Gum/J), Lysm-Cre (B6.129P2-Lyz2tm1(cre)Ifo/J), Vav-iCre (B6.Cg-Commd10Tg(Vav1-icre)A2Kio/J), Cd300lf-/-Cd300ld-/-, BALB/cJ, A/J, NOD/ShiLtJ, 129S1/SvImJ, PWK/PhJ, C57BL/6NCrl, BALB/cAnNCrl.

Mice were used as neonates (postnatal day 6), juveniles (postnatal day 15), or as adults (6-9 weeks). Animals are housed up to five adult mice in a cage or a single dam with a lactating litter. Temperatures are maintained between 68-72°F and humidity between 30-70%. The room light cycle is 12h light, 12h dark. Age- and sex-matched adults were used in adult mouse infections. Litters of pups including males and females were used in neonatal mouse experiments. Number of mice used in each experiment are shown in figure legends.

Animal protocols were approved by the Washington University Animal Studies Committee IACUC (Institutional Animal Care and Use Committee, protocol numbers 20160126, 20190162, 22-1040).

Wild animals

The study did not involve wild animals

Reporting on sex

Litters used included a mix of male and female neonates. For studies on adult mice, both male and female mice were used.

Field-collected samples

The study did not involve field-collected samples

Ethics oversight

All animal experiments were performed in accordance with federal and university guidelines and approved by the Institutional Animal Care and Use Committee at Washington University of St. Louis.

Note that full information on the approval of the study protocol must also be provided in the manuscript.